Accepted Manuscript

Multiphase response of palynomorphs to the Toarcian Oceanic Anoxic Event (Early Jurassic) in the Réka Valley section, Hungary

Viktória Baranyi, József Pálfy, Ágnes Görög, James B. Riding, Béla Raucsik

Please cite this article as: Baranyi, Viktória, Pálfy, József, Görög, Ágnes, Riding, James B., Raucsik, Béla, Multiphase response of palynomorphs to the Toarcian Oceanic Anoxic Event (Early Jurassic) in the Réka Valley section, Hungary, *Review of Palaeobotany and Palynology* (2016), doi:10.1016/j.revpalbo.2016.09.011

Research paper

Multiphase response of palynomorphs to the Toarcian Oceanic Anoxic Event (Early Jurassic) in the Réka Valley section, Hungary

Viktória Baranyi [a*], József Pálfy [b,c], Ágnes Görög [a], James B. Riding [d], Béla Raucsik [e]

a Department of Palaeontology, Eötvös Loránd University, Pázmány Péter sétány 1/C, Budapest H-1117, Hungary

b Department of Physical and Applied Geology, Eötvös Loránd University, Pázmány Péter sétány 1/C, Budapest H-1117, Hungary

c MTA-MTM-ELTE Research Group for Paleontology, POB 137, Budapest H-1431, Hungary

d British Geological Survey, Environmental Science Centre, Keyworth, Nottingham NG12 5GG, United Kingdom

e Department of Mineralogy, Geochemistry and Petrology, University of Szeged, Egyetem utca 2, Szeged H-6722, Hungary

* Corresponding author. Current address: Department of Geosciences, University of Oslo, POB 1047 Blindern, 0316 Oslo, Norway

E-mail address: viktoria.baranyi@geo.uio.no (V. Baranyi)

1

Abstract

Major palaeoenvironmental and palaeoceanographical changes occurred during the Early

Jurassic Toarcian Oceanic Anoxic Event (T-OAE), due to a perturbation of the global carbon

cycle and a crisis in marine ecosystems. The sequence of environmental change and regional

differences during the T-OAE are not yet fully understood and organic-walled phytoplankton

and other palynomorphs are well-suited, but under-utilised, in research into this event. Based

on quantitative palynological analyses from a black shale-bearing succession at Réka Valley

in the Mecsek Mountains of southwest Hungary, five sequential palynomorph assemblages

are distinguished. These reveal major shifts in organic-walled phytoplankton communities,

driven by palaeoenvironmental changes. In addition, palynofacies analysis helped to

document changes in the composition of sedimentary organic matter, and to quantify the

terrestrial input. Assemblage 1 is characterised by a moderately diverse phytoplankton

community and high levels of terrestrial palynomorphs. Assemblage 2 records a significant

peak of the euryhaline dinoflagellate cyst *Nannoceratopsis*. Assemblage 3 is distinguished by

dominance of highly opportunistic prasinophytes and the temporary disappearance of all

dinoflagellate cyst taxa. Assemblages 4 and 5 represent distinctive phases of a prolonged

recovery phase with low diversity phytoplankton assemblages and intermittently high levels

of terrestrially-derived palynomorphs. The successive disappearance of phytoplankton taxa

and the gradual takeover by opportunistic euryhaline species at the onset of the T-OAE were

related to several phenomena. These include reduced salinity in the surface waters,

establishment of a stable pycnocline and deterioration of nutrient recycling, followed by

oxygen deficiency throughout much of the water column. The high amount of terrestrially-

derived palynodebris indicates intense runoff and freshwater input, driven by the early

Toarcian warming and the enhanced hydrological cycle. Comparison with coeval European

successions proves that the palaeoenvironmental changes during the T-OAE were not entirely

synchronous, and local factors played a crucial role in influencing phytoplankton communities. In the Mecsek Basin, regional freshening of the surface waters and increased terrestrial input due to the proximity of the hinterland had a greater influence on phytoplankton communities compared to the open oceanic setting of the Tethys to the south.

1. Introduction

The early Toarcian (Early Jurassic, ~183–179 Ma) was a time of severe palaeoenvironmental perturbations. Global warming, sea level rise and the associated geochemical changes in the ocean-atmosphere system led to a multiplicity of palaeoenvironmental changes which significantly stressed the biosphere and caused biotic turnovers. Marine transgression, carbon isotope excursions, other geochemical anomalies and widespread deposition of organic-rich sediments are associated with the Toarcian Oceanic Anoxic Event (T-OAE) (Jenkyns, 1988; McArthur et al., 2000; Schouten et al., 2000; Jenkyns et al., 2002; Bailey et al., 2003; van de Schootbrugge et al., 2005a; Hesselbo et al., 2007; Suan et al., 2008; Littler et al., 2009; Korte and Hesselbo, 2011; Hermoso et al., 2013). A plausible initial triggering mechanism for the palaeoenvironmental perturbations is methane hydrate dissociation (Hesselbo et al., 2000; 2007). However the most likely, and less debated, main cause of these paleoenvironmental changes was the emplacement of the Karoo-Ferrar large igneous province (Pálfy and Smith, 2000; McElwain et al., 2005; Svensen et al., 2007; Suan et al., 2008; Burgess et al., 2015).

3

The T-OAE is associated with a minor mass extinction in several taxonomic groups (e.g. Harries and Little, 1999; Pálfy and Smith, 2000; Wignall, 2001; Caruthers et al. 2013; Caswell and Coe, 2013; Danise et al., 2013). Coeval environmental perturbations include increased terrestrial input due to enhanced weathering and riverine influx, stratification of the water column with subsequent anoxia and ocean acidification. These changes caused severe stress for many phytoplankton groups. The effects of oceanic anoxic events on phytoplankton assemblages have been discussed extensively (Bucefalo Palliani et al., 1998; 2002; Bucefalo Palliani and Riding 1999a; Erba, 2004; Mattioli et al., 2004; 2009; van de Schootbrugge et al., 2005b; 2013). Dinoflagellate cysts are one of the major groups of Early Jurassic fossilisable phytoplankton. The dinoflagellates are a diverse eukaryotic protistan group of extant unicellular phytoplankton, and are important primary producers at the base of the marine and freshwater food chains (Taylor et al., 2008). Many dinoflagellates have at least two distinct stages in their life cycle. During the motile stage, they inhabit the photic zone and their distribution is affected mostly by surface water temperature, salinity, nutrient availability and light penetration (Marret and Zonneveld, 2003). Many dinoflagellates include a fossilisable resting cyst in their life cycle; these hypnozygotic cysts are extremely useful in studies of Mesozoic and Cenozoic biostratigraphy, palaeobiology and palaeoecology (Stover et al., 1996). Cyst-producing dinoflagellates are very sensitive to ecological conditions, especially oxygen availability in the bottom waters due to the benthic habitat of the resting cysts (Wall et al. 1977; Anderson et al., 1987). Therefore, due to the planktonic and benthic stages in their life cycle, dinoflagellate cysts provide information on the ecological conditions and physico-chemical properties of both the surface and bottom waters.

Many studies on Early Jurassic dinoflagellate cyst assemblages have focused on their biostratigraphy, palaeobiogeography and taxonomy, (e.g. Gocht, 1964; Davies, 1985; Prauss, 1989; Feist-Burkhardt and Wille, 1992; Riding and Thomas, 1992; Bucefalo Palliani and

Riding 2003a). Palynological aspects of the T-OAE have been discussed by Loh et al. (1986), Prauss (1996), Bucefalo Palliani et al. (1998; 2002), Bucefalo Palliani and Riding (1999a) and van de Schootbrugge et al. (2005b; 2013). These studies aimed to reconstruct the palaeoenvironmental changes associated to the T-OAE using calcareous nannoplankton, dinoflagellate cysts and other organic-walled microplankton groups. The environmental stress that accompanied the T-OAE led to a turnover of dinoflagellate cysts (Bucefalo Palliani and Riding 1999b; Bucefalo Palliani et al., 2002). The genera *Luehndea* and *Umbriadinium,* together with many species either became extinct or temporarily disappeared (Bucefalo Palliani and Riding, 2003a; 2003b).

The objective of this study is to analyse the changes in organic-walled phytoplankton groups (i.e. dinoflagellate cysts and prasinophytes), together with changes in the input of terrestrially-derived material, in a black shale-bearing sequence in the Mecsek Mountains of southwest Hungary. Our principal aim is to reconstruct the pattern of biotal turnover associated with the T-OAE. Comparing microplankton turnover patterns from other localities from the Boreal Realm (e.g. Germany, UK) and the Tethyan Realm (e.g. central Italy), we attempt to elucidate regional and global trends in organic-walled phytoplankton community change and to assess the overprint of regional palaeogeographical effects on global phenomena. In addition, building on previous studies such as Dybkjær (1991), Tyson (1993; 1995), Feist-Burkhardt et al. (2008) and Götz et al. (2008), we record and interpret changes in palynofacies patterns during the T-OAE.

2. Geological setting

The Mecsek Mountains are situated in the southwestern part of the Pannonian Basin in Hungary (Fig. 1A). They form the only exposed part of the Mecsek Zone structural unit that

5

belongs to the Tisza Mega-unit (Fig. 1B; Csontos and Vörös, 2004; Haas and Péró, 2004). The Tisza Mega-unit consists of tectonic blocks of the European Plate that were accreted during the Variscan orogeny, and broke off the southern margin of the European Platform (Fig. 2). It reached its present position after a series of drifting and rotation events during the Paleogene and Neogene (Csontos et al., 1992; 2002).

During the Triassic and Early Jurassic, the Mecsek Basin was located east of the Bohemian Massif, and was an epicontinental depocentre (Fig. 2; Haas and Péró, 2004). The Mecsek Basin was situated close to the continental margin, and was therefore exposed to significant terrigeneous influence (Bleahu et al., 1994). The Upper Triassic to lowermost Jurassic succession is characterised by fluvial, lacustrine, coal-bearing swamp and deltaic deposits of the Mecsek Coal Formation (Fig. 3; Szente, 2012). The early Sinemurian eustatic sea level rise coincided with rapid subsidence of the Mecsek Basin, and led to a decrease of terrigenous input and deepening of the depositional environment, as reflected by the Vasas Marl Formation (Fig. 3; Császár et al., 2007; Raucsik, 2012a). During the late Sinemurian and Pliensbachian, terrigeneous material mixed with biogenic carbonate was deposited in this open marine, relatively deep basin and formed an intensely bioturbated lithofacies, assigned to the Hosszúhetény Calcareous Marl Formation (Fig. 3). This unit is informally known as spotted marl, and it is the equivalent of *Fleckenmergel* or *Allgäu* facies elsewhere in the European margin of the Neotethys (Adámek, 2005; Horváth and Galácz, 2006; Raucsik, 2012b). Interbedded bituminous limestones, crinoidal limestones and turbiditic sandstones occur within the monotonous Upper Pliensbachian hemipelagic spotted marl succession, suggesting variable controls on climate change, sea level fluctuations and tectonism (Raucsik and Varga, 2008a). The organic-rich silty and clayey marls of the lower Toarcian Rékavölgy Siltstone Formation mark the establishment of suboxic/anoxic conditions in the Mecsek Basin (Fig. 3; Raucsik, 2012c). The T-OAE is represented by a ~12 m thick black shale succession

6

(Dulai et al., 1992; Raucsik, 2008, 2012c). Overlying the black shales, sedimentation of the spotted marl resumed and continued through to the latest Bajocian Komló Calcareous Marl Formation (Fig. 3; Raucsik, 2012d). Marked sedimentological changes took place in the Mecsek Basin during the Middle Jurassic. The amount of terrigeneous input dramatically decreased. This, together with accelerated subsidence, led to the formation of a deep pelagic basin marking the separation of the Tisza Mega-unit from the European Plate due to the opening of the Penninic oceanic branch (Horváth and Galácz, 2006).

3. The stratigraphy of the Réka Valley section

Jurassic strata are exposed in the eastern part of the Mecsek syncline (Figs. 1A,B; Némedi Varga, 1998). The section studied is located near the NE-SW trending Réka Valley, south of Óbánya (Fig. 4). The ~12 m thick black shale succession crops out in a small tributary ravine. The section was described in detail by Galácz (1991), Dulai et al. (1992) and Raucsik and Varga (2008a; 2008b). The lower part of the section exposes a rhythmic succession of intensely bioturbated calcareous and clayey marl beds (spotted marl) with intercalations of mixed carbonate-siliciclastic lenses (Fig. 5). The spotted marl succession is interrupted by a black shale unit which consists of light brown to dark grey bituminous shale and greyish clayey marl layers with distinct lamination at some levels, with bivalves, fish, plant fragments, and common pyrite framboids and moulds (Dulai et al., 1992; Raucsik, 2008). Intercalations of calcareous-siliciclastic turbidite beds occur in the upper part of the black shale unit, above which is more spotted marl facies (Fig. 5).

The ammonites *Hildaites* cf. *gyralis, H*. cf. *levisoni* and *H*. cf. *siemensi* in the black shales, together with *Harpoceras* cf. *exaratum* from directly above the uppermost black shale beds, indicate the lower Toarcian *Harpoceras falciferum* ammonite biozone (Galácz, 1991).

7

However, due to the somewhat sporadic occurrence of ammonites, the base of the Toarcian, and the boundary between the *Dactilyoceras tenuicostatum* and *H. falciferum* ammonite biozones remain poorly constrained (Galácz, 1991; Dulai et al., 1992; Baldanza et al., 1995; Varga et al., 2009). Based on calcareous nannoplankton, Baldanza et al. (1995) suggested that the boundary between the *D. tenuicostatum* and *H. falciferum* ammonite biozones may lie several metres above the base of the black shale (Fig. 5). In sample BS 15 (1 m below sample BS 16), Mattioli in Varga et al. (2009) encountered the calcareous nannoplankton species *Carinolithus poulnabronei*, which often occurs together with *C. superbus* in early Toarcian assemblages, and indicates the *D. tenuicostatum* ammonite biozone. Sample BS 59 (1 m above sample BS 58) yielded *Watznaueria colacicchii* and *W. fossacincta*. The first appearances of these species are normally coincident with the inception of *Discorhabdus striatus*, indicating correlation with the uppermost part of the *H. falciferum* ammonite biozone (Mattioli and Erba, 1999). The dinoflagellate cyst assemblages of the Réka Valley section were studied by Baldanza et al. (1995) and Bucefalo Palliani et al. (1997), who focussed on biostratigraphy, palaeogeography and taxonomy. The species *Luehndea cirilliae* and *L. microreticulat*a were first described from the Réka Valley section by Bucefalo Palliani et al. (1997).

The total organic carbon (TOC) values of the strata studied vary from 3.89 to 8.12% in the black shales, and 2.14 to 3.29% in the marls (Varga et al., 2007). Investigation of samples from the lower 5 m of the black shale succession show that the organic macerals are virtually all liptinite, and are mainly marine-derived (Varga et al., 2007). The carbon isotopic composition of the kerogen ranges from -30.9‰ to -28.6‰ relative to V-PDB (Varga et al., 2007). These values are slightly less negative than in other Toarcian organic-rich formations, yet strongly suggest a correlation with the characteristic carbon isotope excursion of the T-OAE (Jenkyns et al., 2002). The carbon and oxygen isotopic composition of the carbonate

8

fraction has been altered diagenetically, therefore they cannot be used in palaeoenvironmental interpretations (Varga et al., 2007). The clay minerals in the black shales are dominated by kaolinite (Raucsik and Varga, 2008a; 2008b), which is typical of strongly leached soils that have become progressively enriched in aluminium (van de Schootbrugge et al., 2009). This indicates extremely high continental weathering rates in the source area related to humid, tropical-subtropical climatic conditions (Branski, 2010).

4. Material and methods

Thirty-five samples, BS 2–58, from the Réka Valley section were analysed herein (Fig. 5). Palynomorphs from this black shale succession were extracted from these horizons, which is the same sample set as in Varga et al. (2007) and Raucsik and Varga (2008a, 2008b). Additional palynology samples were collected from the strata underlying and overlying the black shale; these were numbered RV 1–20.

All the samples were prepared using the standard palynological processing techniques of Wood et al. (1996), including treatment with concentrated HCl and HF for the dissolution of carbonate and silicate minerals respectively. For density separation, $ZnCl_2$ solution (density 2.2 g/cm^3) was used. To reduce amorphous organic matter (AOM), black shale samples were oxidised using either NaOH, a mixture of NaOH and HNO_3, or Schulze's solution (a mixture of an aqueous solution of $KClO_3$ and concentrated HNO_3). To avoid the loss of small (~20 μm) palynomorphs, the organic residues were not sieved. Microscope slides were mounted using glycerine jelly.

The relative percentage of palynomorphs is based on counts of ~200 grains and using up to four microscope slides. Sample RV 5 proved barren, and samples BS 48, BS 46, BS 44, RV 17, RV 19 and RV 20 were palynologically sparse; i.e. <30 specimens were recovered. Dinoflagellate cysts were relatively low in diversity and moderately well preserved. By

9

contrast, the terrestrially-derived palynomorphs were highly diverse and generally well preserved with a colouration index of 1 to 2 using the thermal alteration scale of Batten (2002). The relative abundance of palynomorphs was calculated and plotted using Tilia/TiliaGraph software (Grimm, 1991–2001). The palynomorph assemblages were defined using constrained cluster analysis using CONISS (Grimm, 1987) within Tilia (Fig. 6).

Palynofacies analysis was undertaken to determine the type and preservation of the sedimentary organic matter, and the amount of terrigenous input. The subdivision and terminology of the kerogen types follows Oboh-Ikuenobe and de Villiers (2003) (see Table 1). Four palynofacies parameters were calculated on the basis of counting ~400 organic grains per slide. These were: the ratio of terrestrial to marine palynomorphs (t/m); the ratio of spores to bisccate pollen grains (sp/bs); the ratio of opaque to translucent phytoclasts (op/tr); and the ratio of bladder or lath-shaped to equidimensional opaque phytoclasts (bl/eq). This methodology follows Tyson (1993), Pittet and Gorin (1997), Feist-Burkhardt et al. (2008) and Götz et al. (2008) (Fig. 7, Table 1).

Despite multiple oxidation treatments, the black shale samples yielded large amounts of AOM that made the identification of palynomorphs and phytoclasts difficult or impossible. The AOM was analysed under fluorescent light to evaluate the preservational state of the sedimentary organic matter, and to distinguish the palynomorphs and phytoclasts that are masked by the AOM in light microscopy. However, fluorescence microscopy proved unsuitable because of the intense autofluorescence of the glycerine jelly. Furthermore, the intense fluorescent light damages this mounting material. For these reasons, meaningful palynofacies analyses could only be carried out in the underlying and overlying units. Results from the black shale samples are not reliable, and are not used for comparison to the other samples.

Optical microscopy was carried out in the Department of Palaeontology, Eötvös Loránd University, Budapest, Hungary using a Nikon Eclipse E600 microscope. The fluorescence microscopy was undertaken at the Department of Botany, Hungarian Natural History Museum, using a Nikon Eclipse E600 equipped with a fluorescent light source. All samples, residues and microscope slides, including the figured specimens (Plates I–III), are curated at the Department of Palaeontology, Eötvös Loránd University. Palynomorph and palynofacies counts are available as online supplementary material. The nannoplankton samples of E. Mattioli are curated at the Collections de Géologie de Lyon with FSL numbers from 765 965 to 765 996.

Data analysis and calculation of the diversity indices were carried out using the PAST software package 3.01 (Hammer et al., 2001). Samples containing <30 specimens were excluded from the data analyses. For each sample, the diversity of the marine phytoplankton was expressed using the Simpson Diversity Index (1-D). This is a suitable method because the palynomorph abundances are heterogenous. The Simpson Diversity Index takes into account the number of taxa. It ranges between 0 for monospecific assemblages and 1 where all taxa are equally abundant. The index assesses the probability that two individuals randomly selected from a sample will belong to a different taxon, and the greater the 1-D value, the greater the diversity (e.g. Danise et al. 2013). The Simpson Diversity Index was calculated only for the marine taxa because the reconstruction of terrestrial vegetation dynamics is beyond the scope of this study.

Correspondence analysis (CA) and detrended correspondence analysis (DCA) were also performed using the PAST software (Hammer et al., 2001). The square-root transformed data from the marine palynomorph counts were used, as palynological variables are similar to other biological variables and they are not normally distributed, so the standard deviations are

11

often heterogenous (McDonald, 2014). CA and DCA were used to assess similarities between the samples studied to explore relationships between the different marine palynomorph groups (Hill and Gauch, 1980; Kovach, 1993). Special emphasis was placed on the co-occurrences of the different marine palynomorph groups to help identify palaeoecological changes (Correa-Meitro et al., 2014). A taxon abundance matrix was used for the input of data. The first and second axes are displayed both in the CA and DCA plot (Fig. 8). The advantage of DCA compared to other ordination methods is the elimination of the arch effect (Hill and Gauch, 1980; Hammer et al., 2001), and its relative insensitivity to differences in sample size (e.g. palynomorph counts) or diversity (De Toledo et al., 2009). The data matrix, eigenvalues , row and coloumn scores are available as online supplementary material.

5.   Results

5.1.   Palynology, palynofacies and diversity

In this section, the palynomorph assemblages are described in detail. The marine palynomorphs are dominated by dinoflagellate cysts (Plate I). Terrestrially-derived palynomorphs include prominent bisaccate pollen, *Classopollis* sp., non-saccate gymnospermous pollen grains and trilete spores (Plate II). The spores were produced by ferns, lycopods and mosses, and belong to 19 genera. *Cyathidites*, the smooth trilete fern spore genus, is predominant. Ornamented forms are less frequent, although *Ischyosporites variegatus* and *Manumia delcourtii* are sporadically common. Bisaccate pollen is represented by *Alisporites robostus*, *Alisporites* cf. *thomasii*, *Pityosporites* sp. and *Vitreisporites pallidus*. Non-saccate pollen, such as *Cerebropollenites* sp., *Chasmatosporites* spp., *Monosulcites* spp. and *Spheripollenites psilatus*, occur sporadically. The general characteristics of the sporomorphs are similar to other late Pliensbachian to early Toarcian assemblages from Europe (van Erve, 1977; Lund and Pedersen, 1984; Guy-Ohlson, 1986; Dybkjær, 1991;

12

Bucefalo Palliani, 1997). Acritarchs occur throughout, although they are low in both abundance and diversity; only three genera were recognised. Four prasinophyte taxa were distinguished, these include small (10–15 μm in diameter), thin-walled, spherical palynomorphs, referred to as sphaeromorphs, and are characteristic of the black shale samples (Plate III). These have been referred to the prasinophyte species *Halosphaeropsis jurassica* by, for example, Bucefalo Palliani and Riding (2000). On the basis of changes in palynomorph diversity/composition and palynofacies, five assemblages were distinguished using cluster analysis (Fig. 6) and these are described below.

5.1.1. *Assemblage 1 (samples RV 1 to RV 7)*

In this interval, marine palynomorphs are more abundant than spores and pollen. The terrestrial/marine (t:m) index is <1 except in RV 6, where it reaches 1.69 (Figs. 6, 7). The dinoflagellate cyst genus *Luehndea* is dominant. *Luehndea cirilliae* and *L. spinosa* (Plate I, 12) are frequent, whereas *L. microreticulata* (Plate I, 9, 10) is rare. Other dinoflagellate cysts such as indeterminate forms, *Mancodinium semitabulatum*, *Mendicodinium* spp., *Umbriadinium mediterranense* and *Valvaeodinium* spp. are relatively rare. Prasinophytes and sphaeromorphs are minor constituents (3–6%). The Simpson Diversity Index is approximately 0.8, indicating a relatively even species distribution within the phytoplankton (Fig. 6). In the terrestrial fraction, gymnospermous pollen grains are dominant and the kerogen is of mixed marine and terrestrial origin (Plate III, 5). Opaque phytoclasts are dominant (82.5% in average), and palynomorphs are subordinate (Fig. 7).

5.1.2. *Assemblage 2 (samples RV 8 and RV 9)*

Samples RV 8 and RV 9 are characterised by common *Nannoceratopsis,* which represents 99% of the dinoflagellate cysts and 66% of the total palynomorphs (Fig. 6). The

13

Simpson Diversity Index falls to 0.3, suggesting significant assemblage change (Fig. 6).

Nannoceratopsis gracilis exhibits considerable intraspecific variability; some forms have

prominent dorsal antapical horns and strongly reduced ventral antapical horns. Morphotypes

13 and 17 of Gocht (1964) are common. These forms (Plate I, 4, 5) are similiar to *N. gracilis*

subsp. *obsoleta*, which is characteristic in the early Toarcian of Germany (Prauss, 1989).

Some specimens are close to *N. magnicornus* (e.g. Plate I, 11). A few forms with

characteristic rectangular outlines bear prominent dorsal and reduced ventral antapical horns

(Plate I, 6). Specimens with antapical horns of equal length are less frequent. *Luehndea*

spinosa is present in RV 9, this is the stratigraphically highest occurrence of the species in this

section. The range of this species is late Pliensbachian to earliest Toarcian, from the

Pleuroceras spinatum to the *D. tenuicostatum* ammonite biozone (Bucefalo Palliani et al.,

1997). The abundance of the sphaeromorphs increased. The t:m index is low, between 0.06

and 0.25, but in the terrestrial fraction, the ratio of spores to bisaccate pollen is higher

compared to Assemblage 1 (2.75 and 1.00 respectively) (Fig. 7). The relative proportion of

trilete spores and *Classopollis* spp. to bisaccate pollen grains is higher than in Assemblage 1.

Opaque phytoclasts of various shapes and sizes are the dominant kerogen maceral (Plate III,

6). Equidimensional and lath-shaped particles are both present (Fig. 7) and amorphous

organic matter is absent.

5.1.3. Assemblage 3 (samples BS 2 to BS 59)

In the samples from the black shale, the abundance of all palynomorphs declined sharply

except the sphaeromorphs which dominate this assemblage, comprising 93% of the total

palynomorph assemblage (Fig. 6). The Simpson Diversity Index values are extremely low,

ranging from 0.04 to 0.33. Sample BS 32, with a relatively high Simpson Diversity Index, is

characterised by a moderately high diversity of prasinophytes, including species of

14

Tasmanites and sphaeromorphs. Other prasinophytes are *Cymathiosphaera pachytheca*, *Leiosphaeridia* sp. and *Pleurozonaria polyporosa*. The sphaeromorphs occur either as single grains, in chains, or in clusters (Plate III, 1, 2). Dinoflagellate cysts are virtually absent in this assemblage; a few poorly-preserved specimens were observed in sample BS 2. Sedimentary organic matter is represented mostly by AOM (Plate III, 3, 4). This is homogenous using plain transmitted light, but fluorescence reveals that the AOM commonly obscures phytoclasts, prasinophytes, sphaeromophs and sporomorphs (Plate III, 3). The fluorescence of the AOM is very weak, from pale brown to yellowish green, in marked contrast with the brightly fluorescent, yellow to green coloured palynomorphs and phytoclasts (Plate III, 3, 4).

5.1.4. Assemblage 4 (samples RV 10 to RV 15)

The terrestrial fraction of Assemblage 4, in the beds immediately overlying the black shale, abruptly increases. In samples RV 11 to RV 15 the ratio of trilete spores, such as *Cibotiumspora jurienensis, Concavisporites mesozoicus, Cyathidites* spp*., Dictyophyllidites harrisii* and *Ischyosporites variegatus,* increases significantly, associated with abundant terrestrial phytoclasts (Figs. 6, 7). The spore/bisaccate pollen ratio ranges from 5.0 to 5.5. The microplankton assemblages are very sparse; acritarchs and dinoflagellate cysts are rare. Their scarcity may be due to the diluting effect of phytoclasts and sporomorphs. Dinoflagellate cysts are represented by rare *Nannoceratopsis senex* (Plate I, 1). Prasinophycean algae are common, and sphaeromorphs still occur in significant numbers (average 83%). However, they show a decreasing trend from samples RV 10 to RV 12, and they do not occur in chains or clusters. The t/m index remains low, as the sphaeromorphs are still common. Small aggregates of AOM are present in samples RV 13 to RV 15, but it is absent in the rest of the samples. Translucent phytoclasts, which exhibit a great variety of colour, shape and size, are dominant in the kerogen assemblages (Fig. 7).

15

5.1.5. Assemblage 5 (samples RV 16 to RV 20)

The palynomorph spectrum from the uppermost assemblage is dominated by terrestrial input, hence the marine fraction is somewhat impoverished (Fig. 6). Dinoflagellate cysts comprise ~4% of the marine palynomorphs throughout. The first occurrence of *Nannoceratopsis spiculata* (Plate I, 13) is in sample RV 20; this permits a correlation to the *Hildoceras bifrons* ammonite biozone (Riding and Thomas, 1992). The proportion of acritarchs (6%) is higher than in Assemblage 4. The Simpson Diversity Index of the phytoplankton does not approach the levels of values Assemblages 1 and 2 (Fig. 6). Prasinophytes occur in significant numbers (21%), but sphaeromorphs are absent. Sporomorphs dominate the assemblages, with spores being most abundant. The sporomorphs from Assemblages 4 and 5 are relatively conservative, however, the ratio of bisaccate pollen to trilete spores is higher in Assemblage 5 compared to Assemblage 4 (Figs. 6, 7). Palynofacies allows the two assemblages to be separated. Opaque, equidimensional phytoclasts increase in abundance, and AOM is absent throughout in Assemblage 5 (Plate III, 7, 8). The relative proportions of marine material are higher than in Assemblage 4, but the t/m index is also high with an average of 4.3, reflecting the impoverished phytoplankton communities.

5.2.   Multivariate statistical analysis

To analyse the palaeoecological signals which controlled the succession of palynomorph assemblages, multivariate ordination methods, correspondence analysis (CA) and detrended correspondence analysis (DCA) were performed on the palynomorph data (Fig. 8). Using CA, Axis 1 elucidates 58% of the total variance within the dataset, whereas Axis 2 carries an additional 24% of the variance (Fig. 8A). In the DCA analysis, the elimination of the arch

16

effect by division of the ordination into segments distorts the variance fractions. Therefore the

eigenvalues of the different axes cannot be interpreted as variance fractions (Hill and Gauch,

1980; Legendre and Legendre, 1998). The eigenvalues, by contrast, reflect the relative

importances of the different axes (Legendre and Legendre, 1998; Correa-Metrio et al., 2014),

and higher values account for more variance within the data. In this case Axis 1 is similar to

the CA plot with an eigenvalue of 0.5842, compared to the significantly lower eigenvalue of

0.1638 for Axis 2 (Fig. 8B)

In both the CA and DCA scatter plots, four major groups of samples are distinguished

(Fig. 8). These generally correspond to the palynomorph assemblages established herein,

except that Assemblages 3 and 4 could not be separated due to the predominance of

sphaeromorphs. Assemblages 1 and 3–4 are strongly polarised in both plots along Axis 1 (Fig.

8). The similarity of Assemblages 1 and 5 is demonstrated by their proximity in the plots, but

they exhibit clear separation from Assemblage 2 (Fig. 8).

6. Discussion

6.1. Successive change of the phytoplankton communities

The palynological analyses of the Réka Valley section indicates that the phytoplankton

communities responded to the palaeoenvironmental stress associated with the T-OAE by the

successive replacement of characteristic assemblages. In order to explore this further, the

succession was divided into five palynomorph assemblages (Fig. 6) which represent distinct

intervals during the progression of this major palaeoenvironmental perturbation. These

intervals reflect changes in the paleocommunities that can be interpreted using the framework

of four successive stages recognised in modern ecosystems affected by hypoxia. These

include: (0) severely disturbed communities; (1) disturbed communities; (2) transitional

17

communities; and (3) undisturbed, climax communities (Diaz and Rosenberg, 2008). Three of these (communities 0 to 2) are unequivocally present in the Réka Valley succession, and are described below

6.1.1.   Interval 1

The most abundant dinoflagellate cysts, *Luehndea spinosa* and *Nannoceratopsis gracilis,* are interpreted as being opportunistic species, which may have favoured elevated nutrient levels as a result of high terrigenous input (Bucefalo Palliani and Riding 1997a,b; 2000). The assemblage in Interval 1 has the highest Simpson Diversity Index values (0.7–0.85) within the entire succession (Fig. 6). Interval 1 represents a transitional phase (community 2 of Diaz and Rosenberg, 2008) from an undisturbed, climax community to a disturbed association (Assemblage 2). This is manifested by an increasing number of opportunistic species, and higher bioproductivity. A true undisturbed, climax community (community 3 of Diaz and Rosenberg, 2008) was not encountered in the succession studied, because all the assemblages were characterised by moderate to low diversities, and high abundances.

A warm, humid palaeoclimate and significant riverine influx are inferred from the presence of spores such as *Cibotiumspora juriensis, Cyathidites* spp., *Dictyophyllidites harrisii, Ischyosporites variegatus, Manumia delcourtii, Neoraistrickia* sp. and *Uvaesporites argentaeformis*. These were often associated with riverine settings or, warm and wet marsh environments (Abbink et al., 2004). Additionally, spore spikes are often associated with global warming, acceleration of the hydrological cycle and carbon cycle perturbation as demonstrated for the end-Triassic event (Bonis et al., 2009). The strong heterogeneity of phytoclasts (e.g. brown wood, charcoal, cortex, cuticle fragments and membranous tissues), shape and size (Fig. 7) is also explained by intense riverine input resulting from enhanced runoff from the hinterland (Dybkjær, 1991). The Réka Valley section had a more distal

depositional setting compared to Denmark, Germany or the UK and there is no evidence for sea-level drop in the early Toarcian that could have contributed to increased terrestrial input (Galácz, 1991). Therefore the high phytoclast counts and the heterogeneity of the group are assigned to increased runoff rather than shorter transport or prioximity of the hinterland.

This scenario is consistent with the ongoing global warming and increasing humidity, intensification of continental weathering and enhanced runoff from the hinterland during the early Toarcian (McElwain et al., 2005; Dera et al., 2009). The shift towards increased humidity, continental weathering and runoff is also supported by the high kaolinite content in the clay mineral spectrum of the Réka Valley succession (Raucsik and Varga, 2008a,b). The absence of AOM indicates ventilated, well-oxygenated bottom conditions and vertical mixing of nutrients in the water column. In summary, strong terrestrial influence and eutrophic conditions are inferred from the palynofacies and the palynomorph distribution in Interval 1.

6.1.2. Interval 2

The abundance of *Nannoceratopsis* spp. in Interval 2 indicates significant disturbance of the phytoplankton communities. The opportunistic, euryhaline character of this genus (Riding, 1983; 1984; 1987; Riding et al., 1985) readily allows adaptation to lower salinity conditions in the surface waters caused by increased freshwater input. The low Simpson Diversity Index values (0.3–0.5) (Fig. 6) also suggest that this assemblage represents a disturbed community (community 1 of Diaz and Rosenberg, 2008). Several aberrant morphotypes of *Nannoceratopsis gracilis* occur in Interval 2. Some of these are similar to *N. magnicornus* (see Bucefalo Palliani and Riding, 1997a); others resemble *N. gracilis* subsp. *obsoleta* (see Prauss, 1989). However, others exhibit a rectangular outline and one prominent dorsal antapical horn (Plate I, 6.). These morphotypes are confined to Interval 2. In Interval 1,

19

Nannoceratopsis is represented by different species. The appearance of these unusual forms is indicative of stressed palaeoenvironments, and represents the reaction of this genus to lower surface water salinity and/or changes in oxygen and nutrient availability. According to Bucefalo Palliani and Riding (2000), these unusual morphological features of *Nannoceratopsis* reflect the differing tolerance levels of the species. *Nannoceratopsis magnicornus* did not survive the anoxic phase in England, France and Hungary, whereas *N. gracilis* and *N. senex* are still present in higher stratigraphical levels at these localities. It is difficult to determine the adaptational advantages or disadvantages of the morphological features of *N. gracilis, N. magnicornus* or *N. senex*. The main control was probably the relationship of size, shape and weight of the cysts to the buoyancy and hydrodynamic forces in stratified water bodies. Evitt (1961) pointed out the huge intraspecific morphological variability of *N. gracilis,* and we suggest that the aberrant forms herein are all different morphotypes of *N. gracilis*. Additionally, studies on many modern dinoflagellates have shown that salinity exerts a strong control on the morphology of their cysts (Ellegaard, 2000; Rochon et al., 2009; Mertens et al., 2012; Verleye et al., 2012). Intringuingly, Evitt (1961) and Gocht (1972) pointed out the similarities of the epicystal tabulation pattern between peridinoid dinoflagellates and *Nannoceratopis*. Although *Nannoceratopsis* belongs to a separate order of dinoflagellates (Fensome et al., 1993) without any modern descendants, it cannot be entirely excluded that they had similar lifestyles to modern peridinoid heterotrophic dinoflagellates (Evitt, 1961), thereby explaining their high productivity and prevalence in eutrophic water masses.

6.1.3. Interval 3

The increased freshwater supply during Intervals 1 and 2 led to the establishment of a stable and stratified water column with dysoxic, or anoxic, conditions at the sea bed and in the

water column. The onset of black shale sedimentation is coeval with a sharp reduction in phytoplankton diversity. The severe disturbance of the phytoplankton communities is manifested by the low Simpson Diversity Index, which dropped from 0.3–0.5 to 0.05–0.2 (Fig. 6). This assemblage represents a severly disturbed community (community 0 of Diaz and Rosenberg, 2008). The low salinity, oxygen-poor and subsequently oligotrophic conditions were only tolerated by some phytoplankton groups. Sphaeromorphs, which dominate the marine palynomorph spectrum, were previously believed to belong to several groups (e.g. green algae, pollen), and their affinity still remains uncertain (Bucefalo Palliani et al. 2002; van de Schootbrugge et al. 2005b; 2013). According to Prauss and Riegel (1989), their affinity is probably the Prasinophyceae, a primitive group of Chlorophyta. This is corroborated by their common co-occurrence with prasinophyte phycomas (van de Schootbrugge et al., 2013). The sphaeromorphs, together with other prasinophytes, are the only phytoplankton groups that could have survived significant freshening of the surface waters. Alternatively, they could withstand periods when dysoxic-anoxic, probably even euxinic, conditions reached the photic zone. Furthermore, they were better adapted to the reduced recycling of nutrients that sank to the bottom, and could not return to the photic zone due to density stratification of the water column (Farrimond et al., 1989; Prauss, 2007).

The extension of the oxygen minimum zone severely affected the dinoflagellate cyst assemblages. Studies on modern dinoflagellates have proved that oxygen availability exerts a strong control on excystment, and anoxic conditions completely prohibit the successful germination of the cysts (Anderson et al., 1987; Pross, 2001). This led to the temporary disappearance of dinoflagellates, a 'blackout' event (Loh et al., 1986).

The abundance of AOM and a lack of bioturbation indicate oxygen deficiency at the sediment-water interface. This lead to the deposition of finely laminated, organic-rich black

21

shales. The kerogen in the black shale consists mainly of marine organic material of algal

origin (liptinite), with less than 10% terrestrial components (vitrinite and intertinite) (Varga et

al., 2007). However, fluorescence analysis reveals that the AOM masks many sporomorphs

and phytoclasts. The temporary presence of euxinic conditions during the deposition of the

black shale in the Réka Valley is manifested by the presence of micrometre-scale pyrite

framboids in the black shale. The episodic return of oxygenated conditions is suggested by

sparse bivalves in the black shale (Galácz, 1991). However, based on the estimates of Röhl

and Schmid-Röhl (2005) from the Posidonia Shale, these episodes may have lasted only few

months or years.

Such a characteristic association of abundant sphaeromorphs and AOM, together with the

lack of dinoflagellate cysts, is widely recognised from the lower Toarcian black shale facies in

northwest Europe (Wall, 1965; Wille, 1982; Lund and Pedersen, 1984; Prauss and Riegel

1989; Dybkjær, 1991; Prauss et al., 1991; Bucefalo Palliani et al., 2002). The dinoflagellate

cyst diasappearance extends from the upper part of the *D. tenuicostatum* to the *H. falciferum*

ammonite biozones. The prasinophytes are considered to be 'disaster taxa' because of their

peaks in the near absence of other phytoplankton groups such as dinoflagellates (van de

Schootbrugge et al., 2005b). However, the reasons for their proliferation during anoxic events,

including their widespread distribution at the T-OAE, are still controversial. Prauss (2007)

summarised the probable causes of prasinophyte abundance during anoxic events (e.g. the T-

OAE and the Cenomanian/Turonian event). He suggested that the low salinity of surface

waters and the extension of the oxygen minimum zone alone cannot account for the turnover

in the phytoplankton communities. Furthermore, the availability of trace elements (Cu, Fe,

Mn, Mo, Zn) and nutrients (N, P) may exert a larger control on different algal groups

(Falkowski et al, 2004; Katz et al., 2004). In addition, the prasinophyte abundance may also

be connected to the denitrification of the water column (Jenkyns et al., 2001).

22

6.1.4. Intervals 4 and 5

The return of bioturbated sediments, such as marls with increasing carbonate content upsection, in the upper part of the section marks the end of the anoxic event, and the re-establishment of an oxygenated water column. However the phytoplankton communities were not yet fully recovered, and represent a disturbed, transitional community to climax assemblages (community 2 of Diaz and Rosenberg, 2008). The Simpson Diversity Index of the phytoplankton continued to remain low (Fig. 6). The Lazarus effect (Wignall and Benton, 1999) is a common feature among the dinoflagellate cysts returning in this interval, because there are many species which reappeared after the event. The adaptation of *Nannoceratopsis* to a more proximal setting with lower salinities may have favoured their survival during the T-OAE. They probably used proximal settings as refugia. Prauss (1996) suggested they could thrive in nearshore palaeoenvironments due to their euryhaline nature (Riding, 1983; 1984; 1987).

This interval is also characterised by an increase of fern spores, whereas other terrestrial palynomorphs occur only in low proportions. This indicates humid and warm palaeoclimatic conditions. Sparse dinoflagellate cysts (e.g. *N. senex*) and acritarchs occur, and sphaeromorphs are still present. The absence of AOM indicates a ventilated, non-stratified water column. The palynofacies is dominated by cuticles, elongated (blade-like) phytoclasts and plant tissues indicating either proximity to the shoreline, intense runoff or both. In Interval 5, sphaeromorphs further declined, and the palynofacies patterns indicate an unstable water column with ventilated conditions. The abundance of predominantly rectangular, small opaque phytoclasts indicates a deepening trend in the late Toarcian of the Mecsek Basin which is consistent with basin evolution in this area (Csontos and Vörös, 2004).

6.2. Multivariate statistical analysis and palynomorph community change

23

A key feature of the scatter plots is the grouping and polarisation of samples along both axes. The fact that changes along Axis 1 account for the majority of variance in the dataset, both in CA and DCA (Fig. 8), implies that the underlying palaeoenvironmental parameter was the main driver of the community replacement of organic-walled microplankton. This is also suggested by the marked difference in the axis scores of dinoflagellate cysts and acritarchs compared to those of sphaeromorphs and prasinophytes (online supplementary material). The similar values for prasinophytes and sphaeromorphs on both axes in the CA and DCA plots indicate a possible relationship, as proposed by Prauss and Riegel (1989), Bucefalo Palliani et al. (2002) and van de Schootbrugge et al. (2005b; 2013). Among the dinoflagellate cysts, *Luehndea* and *Nannoceratopsis* favoured high nutrient levels, approaching eutrophic conditions (Bucefalo Palliani and Riding, 1999a). However, *Luehndea* differs from *Nannoceratopsis* in its lower tolerance of reduced surface salinities. *Nannoceratopsis* is known to be a euryhaline genus, which could have tolerated low surface salinities (Riding, 1983; 1984; 1985; 1987; Prauss, 1996). Samples from Assemblage 1 with high proportion of *Luehndea* plot closer to samples with acritarchs and other dinoflagellate cysts along Axis 1, indicating similar palaeoecological preferences and a more diverse community compared to other intervals. Favourable conditions, ventilated bottom waters and sufficient amount of nutrients are inferred, whereas Assemblages 3 and 4 indicate severe palaeoenvironmental deterioration, i.e. changes in surface water salinity and/or nutrient and oxygen availability. The position of the groups along Axis 1 suggests that it reflects a gradient of stress tolerance of the phytoplankton groups, most likely against adverse changes in nutrient availability in the water column. The assemblages reflect a shift from the eutrophic conditions preferred by *Luehndea* and *Nannoceratopsis* (Bucefalo Palliani and Riding 1999a), to oligotrophic conditions with proliferation of sphaeromorphs due to the establishment of a stratified water column (Bucefalo Palliani and Riding 1999a, Bucefalo Palliani et al. 2002). This gradient

24

may also reflect changes in the type of nutrients available, because green algae (prasinophytes, sphaeromorphs) and dinoflagellates have different nutrient preferences (Falkowski et al. 2004). Additionally, the prevailing hypoxic-anoxic conditions and the probable denitrification of the water column during the T-OAE (Jenkyns et al. 2001) could have favoured the 'disaster taxa' such as the prasinophytes (van de Schootbrugge et al. 2005b; 2013). This also corroborates the hypothesis of Prauss (2007) that low salinity surface waters and oxygen deficiency in the water column alone cannot account for the abundance of the sphaeromorphs during the T-OAE, and that the availability or lack of distinct nutrients exerted a strong control on phytoplankton turnover patterns.

Axis 2 in CA and DCA with the second highest eigenvalues represents another environmental parameter important for the community replacement, which is interpreted here as surface water salinity. Its gradient ranges from normal marine to low salinity surface water, the latter deriving from enhanced riverine freshwater influx. This interpretation is supported by the markedly different scores of the euryhaline genus *Nannoceratopsis* and the other groups on Axis 2 (Fig. 8). This signal may be influenced by the palaeogeographical setting of the Mecsek Basin, as freshwater delivery is only significant in depositional settings close to the continental hinterland, and negligible in the Tethyan open oceanic areas.

7.   Palynostratigraphy

The succession of palynomorph assemblages is also useful for establishing the biostratigraphy of the Réka Valley section. This mainly based on species of the dinoflagellate cyst genera *Luehndea* and *Nannoceratopsis*. The Jurassic dinoflagellate cyst biozonation for northwest Europe was developed by Woollam and Riding (1983), Prauss (1989), Feist-Burkhardt and Wille (1992), Poulsen (1992), Riding and Thomas (1992) and Poulsen and

Riding (2003). The latter zonal scheme can be applied to the the Réka Valley section, where

two dinoflagellate cyst zones can be distinguished. Assemblages 1 and 2 correspond to Zone

DSJ7 of Poulsen and Riding (2003), correlated with the *D. tenuicostatum* ammonite biozone.

The base of this zone is defined by the range tops of *Maturodinium inornatum* and

Valvaeodinium armatum, whereas the top is marked by the apparent extinction of *Luehndea*

spinosa. *Maturodinium inornatum* and *Valvaeodinium armatum* were not recovered here, but

the last occurrence of *L. spinosa* is in sample RV 9. The stratigraphical range of *Luehndea*

extends higher, because *Luehndea cirillae* has been reported from the *H. falciferum* ammonite

biozone (Baldanza et al. 1995; Bucefalo Palliani et al. 1997, Bucefalo Palliani and Riding,

1999b). Assemblage 3 from the black shale unit lacks any age diagnostic dinoflagellate cyst

species, but Assemblages 4 and 5 yielded several specimens of *Nannoceratopsis*, indicative of

Zone DSJ8 of Poulsen and Riding (2003), and correlated with the *H. falciferum* and *H.*

bifrons ammonite biozones.

8.   Correlation and comparison with other lower Toarcian black shale localities

To elucidate regional and global trends in biotic turnovers in organic-walled

phytoplankton communities, four localities were selected for comparison with the five stage

floral replacement pattern observed in the Réka Valley section (Fig. 9). The Brown Moor

borehole in Yorkshire, UK (Bucefalo Palliani et al., 2002), the Bisingen/Zimmern borehole in

southwest Germany (Prauss et al., 1991) and the Grimmen section in northwest Germany

(Prauss, 1996) represent the Northwest European Province. From the Mediterranean Province

of the Tethyan Realm, successions from the Umbria-Marche Basin in central Italy are used

(Bucefalo Palliani et al., 1998; Bucefalo Palliani and Riding, 1999a). In addition, the Quercy

section in southwest France was chosen for comparison due to its transitional position

26

between the epicontinental northwest European and the more open marine Mediterranean regions (Bucefalo Palliani and Riding, 1997a). The characteristic palynological features and the biotic events inferred at these localities are summarised in Fig. 9.

8.1.   *Comparison with northwest Europe*

Marine palynomorphs in the lower Toarcian of northwest Europe are dominated by *Luehndea spinosa*, *Mancodinium semitabulatum*, *Nannoceratopsis* spp., sphaeromorphs and *Tasmanites* spp. (Bucefalo Palliani and Riding, 1999b; 2003a). The Réka Valley assemblages are entirely consistent with this. In North Yorkshire, dinoflagellate cysts are gradually replaced by prasinophytes and sphaeromorphs, resulting in a dinoflagellate cyst blackout event coincident with the negative carbon isotope excursion and the TOC maximum between the *Dactylioceras semicelatum* and *Harpoceras exaratum* ammonite subbiozones (Bucefalo Palliani et al., 2002). By contrast, at Réka Valley, the replacement of dinoflagellate cysts by prasinophytes is sudden rather than gradual, although this may be partly attributed to different sampling resolutions. The duration of the phytoplankton disappearance event and the stratigraphical range of the sphaeromorphs are also longer at Réka Valley.

In the Posidonia Shale of southwest Germany the relative proportions of *Nannoceratopsis senex* increases gradually in the upper part of the *D. tenuicostatum* ammonite biozone to the onset of the bituminous facies, which is comparable to Interval 2 in the Réka Valley section (Fig. 9). The black shale interval in the Posidonia Shale is also devoid of dinoflagellate cysts, similar to Interval 3 at Réka Valley. However, at Grimmen in northwest Germany, *Nannoceratopsis* is present throughout the organic-rich facies (Prauss, 1996). This is due to the more proximal depositional setting and presumabily more effective circulation within the water column at Grimmen, that provided refuge for *Nannoceratopsis.* After the T-OAE, the dinoflagellate cysts returned in the upper part of the *H. bifrons* ammonite biozone in

southwest Germany (Prauss et al., 1991). However, they are less abundant and diverse than before the anoxic event, which is similar to the low phytoplankton levels in Intervals 4 and 5 at Réka Valley. Another similarity between Réka Valley and southwest Germany is the abundance of pollen and spores, together with terrestrial kerogen such as huminite and vitrinite, in the pre-event beds in the *P. spinatum* to *D. tenuicostatum* ammonite biozones (Fig. 9). The replacement of phytoplankton, and the length of the disappearance event, were more pronounced in Germany and the Réka Valley compared to Yorkshire (Fig. 9; Wall, 1965; Prauss and Riegel, 1989; Bucefalo Palliani et al., 2002).

The Quercy succession in southwest France yields similar assemblages to those further north in Europe and the Réka Valley. *Luehndea spinosa* is dominant in the *D. tenuicostatum* ammonite biozone, and the abundance and diversity of *Nannoceratopsis* increases upsection (Bucefalo Palliani and Riding, 1997a). *Nannoceratopsis magnicornus* was described from Quercy, and is also present at Réka Valley (Bucefalo Palliani and Riding, 1997a). The phytoplankton turnover in the higher parts of the lower Toarcian could not be studied at Quercy, because this interval is absent (Bucefalo Palliani and Riding, 1997a).

8.2. *Comparison with the Mediterranean Province*

Mendicodinium spp. are significantly more diverse in the Mediterranean Province than in epicontinental northwest Europe. By contrast, *Luehndea* and *Nannoceratopsis* exhibit greater species richness in the latter province (Riding, 1984; Prauss, 1989; Feist-Burkhardt and Wille, 1992). Furthermore, patterns of community and palaeoenvironmental changes associated with the T-OAE also differ between the two areas (Bucefalo Palliani and Riding, 1999b). The only common features are the apparent extinction of *Luehndea spinosa* before the onset of black shale deposition in the *D. tenuicostatum* ammonite biozone, and the disappearance of dinoflagellate cysts accompanied by a prasinophyte bloom in the organic-rich facies

28

(Bucefalo Palliani et al. 1998; Bucefalo Palliani and Riding, 1999 a,b). There is also an apparent discrepancy in the timing of biotic changes and events between the two provinces. In the Umbria-Marche Basin of central Italy, the onset of the environmental perturbation is recorded in the lowermost *D. tenuicostatum* ammonite biozone, culminating in the middle to upper part of that zone, and the return of oxygenated conditions is in the uppermost part of the *D. tenuicostatum* ammonite biozone (Fig. 9). In Réka Valley, and elsewhere in northwest Europe, the onset of black shale sedimentation and the dinoflagallate cyst disappearance event is higher, i.e. in the uppermost *D. tenuicostatum* to *H. falciferum* ammonite biozones, and the environmental crisis probably extended into the *H. bifrons* ammonite biozone (Prauss et al. 1991). In the Mediterranean region, there is no evidence for elevated terrestrial runoff, freshwater input and the freshening of surface waters, although terrestrial palynomorphs may be sporadically abundant (Bucefalo Palliani, 1997; Bucefalo Palliani and Riding, 1997b). The sphaeromorphs are less significant in the Mediterranean than further north. The palynomorphs in the black shale mainly comprise *Tasmanites* spp. This prasinophyte proliferation may be due to the expansion of the oxygen minimum zone, and the successful nitrogen metabolism of the prasinophytes (Prauss, 2007). Freshening of the surface waters due to riverine influx was negligible in the Tethyan Realm due to its open oceanic setting (van de Schootbrugge et al., 2013). After the end of black shale deposition, phytoplankton recovered rapidly, with new taxa including *Mancodinium semitabulatum, Mendicodinium* spp. and *Susadinium*, which are not present in coeval strata at Réka Valley (Bucefalo Palliani and Riding, 1999a).

9. Conclusions

The palynological and palynofacies analysis of the lower Toarcian black shale-bearing Réka Valley section in southwest Hungary demonstrates significant variations during the T-

29

OAE. The phytoplankton communities responded to the profound environmental stress by exhibiting multiphase change. This has been subdivided into five intervals, with successive reductions in the number of specialist taxa in favour of opportunists. Community replacement was initiated by climate-driven eutrophication and freshening of the surface waters. This lead to maxima (blooms) of the opportunistic dinoflagellate cyst genus *Luehndea* (Interval 1), and subsequently to an acme of the euryhaline dinoflagellate cyst genus *Nannoceratopsis* (Interval 2). The most severe environmental crisis was marked by the dominance of prasinophytes, including sphaeromorphs and *Tasmanites* spp. (Interval 3), indicating reduced nutrient supply and altered physico-chemical conditions of the water column due to water mass stratification. This biotic crisis was followed by a prolonged period of recovery (Intervals 4 and 5).

Comparison of the northwest European and Tethyan Mediterranean provinces in the Toarcian indicates that palaeogeography and regional influences exerted significant control on the composition of phytoplankton communities and turnover patterns. This influenced the dynamics and the extent of the early Toarcian biotic crisis. The five successive stages observed in the Réka Valley succession are consistent with the community replacement pattern documented in epicontinental areas. By contrast, in the Mediterranean Province of the Tethyan Realm, different processes are invoked and there is an apparent temporal discrepancy of biotic events between the two areas. The proliferation of *Nannoceratopsis* is a regional phenomenon in the northwest European Province. It may represent a response to a regional surface water freshening event which did not affect open oceanic settings; neither is it a global phenomenon. The increase in *Nannoceratopsis* was triggered by climatic factors, as warming enhanced continental runoff and increased freshwater influx into the epicontinental basins. However the extinction of the *Luehndea* in the *D. tenuicostatum* ammonite biozone, and a prasinophyte bloom, is recorded both in northwest Europe and the Mediterranean *Luehndea* did not survive the low surface salinity and oligotrophic conditions which became established

30

due to the lack of nutrient recirculation in the photic zone. The intensification of oxygen deficiency, oligotrophic conditions and altered availability of trace elements in seawater all caused the prasinophyte bloom. However in epicontinental areas the freshening of surface waters by riverine input cannot be neglected, and this may have led to the proliferation of this group. These changes are related to large-scale palaeoclimatic and palaeoenvironmental perturbations that were associated with fundamental changes in the ocean-atmosphere system, oceanic current patterns and the physico-chemical parameters of the seawater.

Appendix. List of palynomorph species

This Appendix lists all valid palynomorph taxa below generic level from the Réka Valley section, or mentioned herein, with full author citations. The palynomorphs are listed alphabetically within five groups. References to the dinoflagellate cyst author citations can be found in Fensome and Williams (2004).

Acritarch:

Micrhystridium lymensis Wall 1965

Dinoflagellate cysts:

Luehndea cirilliae Bucefalo Palliani et al. 1997

Luehndea microreticulata Bucefalo Palliani et al. 1997

Luehndea spinosa Morgenroth 1970

Mancodinium semitabulatum Morgenroth 1970

Maturodinium inornatum Morgenroth 1970

Nannoceratopsis gracilis Alberti 1961

Nannoceratopsis gracilis Alberti 1961 subsp. *obsoleta* (Prauss 1989) Lentin & Williams 1993

Nannoceratopsis magnicornus Bucefalo Palliani & Riding 1998

Nannoceratopsis senex van Helden 1977

Nannoceratopsis spiculata Stover 1966

Umbriadinium mediterraneense Bucefalo Palliani & Riding 1997

Valveodinium armatum Morgenroth 1970

Pollen:

Alisporites robustus Nilsson 1958

Alisporites sp. cf. *A. thomasii* (Couper 1958) Nilsson 1958

Chasmatosporites elegans Nilsson 1958

Monosulcites minimus Cookson 1947

Monosulcites subgranulosus Couper 1958

Spheripollenites psilatus Couper 1958

Vitreisporites pallidus (Reissinger 1950) Nilsson 1958

Prasinophytes:

Cymatiosphaera pachytheca Eisenack 1967

Halosphaeropsis liassica Mädler 1963

Pleurozonaria polyporosa Mädler 1963

Spores:

Auritulinasporites triclavis Nilsson 1958

Cibotiumspora jurienensis (Balme 1957) Filatoff 1965

Conbaculatisporites mesozoicus Klaus 1960

Concavisporites toralis (Leschik 1955) Nilsson 1958

Contignisporites problematicus (Couper 1958) Döring 1965

Cyathidites australis Couper 1953

Cyathidites minor Couper 1953

Cyathidites punctatus (Delcourt & Sprumont 1955) Delcourt et al. 1963

33

Dictyophyllidites harrisii Couper 1958

Ischyosporites variegatus Couper 1958

Leptolepidites verrucatus Couper 1953

Manumia delcourtii (Pocock 1970) Dybkjær 1991

Osmundacidites wellmanii Couper 1953

Plicifera delicata (Bolkhovitina 1953) Bolkhovitina 1966

Uvaesporites argenteaeformis (Bolkhovitina 1953) Schulz 1967

References

Abbink, O.A., Van Konijnenburg-Van Cittert, J.H.A., Visscher, H., 2004. A sporomorph ecogroup model for the Northwest European Jurassic–Lower Cretaceous. Concepts and framework. Netherlands Journal of Geosciences 83, 17–38.

Adámek, J., 2005. The Jurassic floor of the Bohemian Massif in Moravia – geology and paleogeography. Bulletin of Geosciences 80, 291–305.

Anderson, D.M., Taylor, C.D., Armbrust, E.V., 1987. The effects of darkness and anaerobiosis on dinoflagellate cyst germination. Limnology and Oceanography 32, 340–351.

Bailey, T.R., Rosenthal, Y., McArthur, J.M., van de Schootbrugge, B., Thirlwall, M.F., 2003. Paleoceanographic changes of the Late Pliensbachian–Early Toarcian interval: a possible link to the genesis of an Oceanic Anoxic Event. Earth and Planetary Science Letters 212, 307–320.

Baldanza, A., Bucefalo Palliani, R., Mattioli, E., 1995. Lower Jurassic calcareous nannofossils and dinoflagellate cysts of Hungary and their comparison with assemblages from Central Italy. Palaeopelagos 5, 161–174.

Bassoulet, J.-P., Elmi, S., Poisson, A., Cecca, F., Bellion, Y., Guiraud, R., Baudin, F., 1993. Middle Toarcian (184–182 Ma.). In: Dercourt, J., Ricou, L. E., Vrielynck, B. (editors), Atlas Tethys Paleoenvironmental Maps. BEICIP-FRANLAB, Rueil-Malmaison, 63–80.

Batten, D.J., 2002. Palynofacies and petroleum potential. In: Jansonius, J., McGregor, D.C. (editors), Palynology: Principles and Applications. American Association of Stratigraphic Palynologists Foundation 3, 1065–1084.

Bleahu, M., Mantea, G., Bordea, S., Panin, S., Ştefănescu, M., Sikić, K., Haas, J., Kovács, S., Péró, Cs., Bérczi-Makk, A., Konrád, Gy., Nagy, E., Rálisch-Felgenhauer, E., Török, Á., 1996. Triassic facies types, evolution and paleogeographic relations of the Tisza Megaunit. Acta Geologica Hungarica 37, 187–234.

Bonis, N.R., Kürschner, W.M., Krystyn, L., 2009. A detailed palynological study of the Triassic–Jurassic transition in key sections of the Eiberg Basin (Northern Calcareous Alps, Austria). Review of Palaeobotany and Palynology 156, 376–400.

Branski, P., 2010. Kaolinite peaks in early Toarcian profiles from the Polish Basin - an inferred record of global warming. Geological Quarterly 54, 15–24.

Bucefalo Palliani, R., 1997. Toarcian sporomorph assemblages from the Umbria-Marche basin, central Italy. Palynology 21, 105–121.

Bucefalo Palliani, R., Cirilli, S., Mattioli, E., 1998. Phytoplankton response and geochemical evidence of the lower Toarcian relative sea level rise in the Umbria Marche basin (Central Italy). Palaeogeography, Palaeoclimatology, Palaeoecology 142, 33–50.

Bucefalo Palliani, R., Mattioli, E., Riding, J.B., 2002. The response of marine phytoplankton and sedimentary organic matter to the early Toarcian (Lower Jurassic) oceanic anoxic event in northern England. Marine Micropaleontology 46, 223–245.

Bucefalo Palliani, R., Riding, J.B., 1997a. The influence of palaeoenvironmental change on dinoflagellate cyst distribution. An example from the Lower and Middle Jurassic of Quercy, southwest France. Bulletin du Centre de Recherches Elf Exploration-Production 21, 107–123.

36

Bucefalo Palliani, R., Riding, J.B., 1997b. Lower Toarcian palynostratigraphy of Pozzale, central Italy. Palynology 21, 91–103.

Bucefalo Palliani, R., Riding, J.B., 1999a. Relationship between the early Toarcian anoxic event and organic-walled phytoplankton in central Italy. Marine Micropaleontology 37, 101–116.

Bucefalo Palliani, R., Riding, J.B., 1999b. Early Jurassic (Pliensbachian–Toarcian) dinoflagellate migrations and cyst paleoecology in the Boreal and Tethyan realms. Micropaleontology 45, 201–214.

Bucefalo Palliani, R., Riding, J.B., 2000. A palynological investigation of the Lower and lowermost Middle Jurassic strata (Sinemurian to Aalenian) from North Yorkshire, UK. Proceedings of the Yorkshire Geological Society 53, 1–16.

Bucefalo Palliani, R., Riding, J.B., 2003a. Biostratigraphy, provincialism and evolution of European Early Jurassic (Pliensbachian to early Toarcian) dinoflagellate cysts. Palynology 27, 179–214.

Bucefalo Palliani, R., Riding, J.B., 2003b. *Umbriadinium* and *Polarella*: an example of selectivity in the dinoflagellate fossil record. Grana 42, 108–111.

37

Bucefalo Palliani, R., Riding, J.B., Torricelli, S., 1997. The dinoflagellate cyst *Luehndea* Morgenroth, 1970, emend. from the upper Pliensbachian (Lower Jurassic) of Hungary. Review of Palaeobotany and Palynology 96, 113–120.

Burgess, S.D., Bowring, S.A., Fleming, T.H., Elliot, D.H., 2015. High-precision geochronology links the Ferrar large igneous province with early-Jurassic ocean anoxia and biotic crisis. Earth and Planetary Science Letters 415, 90–99.

Caruthers, A.H., Smith, P., Gröcke, D.R., 2013. The Pliensbachian–Toarcian (Early Jurassic) extinction, a global multi-phased event. Palaeogeography, Palaeoclimatology, Palaeoecology 386, 104–118.

Caswell, B.A., Coe, A.L., 2013. Primary productivity controls on opportunistic bivalves during Early Jurassic oceanic deoxygenation. Geology 41, 1163–1166.

Correa-Metrio, A., Dechnik, Y., Socorro, L.-G., Caballero, M., 2014. Detrended correspondence analysis: A useful tool to quantify ecological changes from fossil data sets. Boletín de la Sociedad Geológica Mexicana 66, 135–143.

Császár, G., Görög, Á., Gyuricza, Gy., Sieglné Farkas, Á., Szente, I., Szinger, B., 2007. The geological, palaeontological and sedimentological pattern of the Vasa Marl Formation between Zsibrik and Ófalu, South Transdanubia. Földtani Közlöny 137, 193–226.

Csontos, L., Benkovics, L., Bergerat, F., Mansy, J., Wórum, G., 2002. Tertiary deformation history from seismic section study and fault analysis in a former European Tethyan margin (the Mecsek–Villány area, SW Hungary). Tectonophysics 357, 81–102.

Csontos, L., Nagymarosy, A., Horváth, F., Kovác, M., 1992. Tertiary evolution of the Intra-Carpathian area: a model. Tectonophysics 208, 221–241.

Csontos, L., Vörös, A., 2004. Mesozoic plate tectonic reconstruction of the Carpathian region. Palaeogeography, Palaeoclimatology, Palaeoecology 210, 1–56.

Danise, S., Twitchett, R.J., Little, T.S., Clémance, M.-E., 2013. The impact of global warming and anoxia on marine benthic community dynamics: an example from the Toarcian (Early Jurassic). PLOS ONE 8, e56255.

Davies, E.H., 1985. The miospore and dinoflagellate cyst Oppel-zonation of the Lias of Portugal. Palynology 9, 105–132.

Dera, G., Pellenard, P., Neige, P., Deconinck, J.-F., Pucéat, E., Dommergues, J.-L., 2009. Distribution of clay minerals in Early Jurassic Peritethyan seas: Palaeoclimatic significance inferred from multiproxy comparisons. Palaeogeography, Palaeoclimatology, Palaeoecology 271, 39–51.

De Toledo, M.B., Barth, O.M., Silva, C.G., Barros, M.A., 2009. Testing multivariate analysis in paleoenvironmental reconstructions using pollen records from Lagoa Salgada, NE Rio de Janeiro State, Brazil. Annals of the Brazilian Academy of Sciences 81, 757–768.

Diaz, R.J., Rosenberg, R. 2008. Spreading dead zones and consequences for marine ecosystems. Science 321, 926–929.

Dulai, A., Suba, Z., Szarka, A., 1992. Toarcian (Lower Jurassic) organic-rich black shale in the Réka valley (Mecsek Hills, Hungary). Földtani Közlöny 122, 67–87.

Dybkjær, K., 1991. Palynological zonation and palynofacies investigation of the Fjerritslev Formation (Lower Jurassic–basal Middle Jurassic) in the Danish Subbasin. Danmarks Geologiske Undersøgelse Serie A, Nr. 30, 150 p.

Ellegard, M., 2000. Variations in dinoflagellate cyst morphology under conditions of changing salinity during the last 2000 years in the Limfjord, Denmark. Review of Palaeobotany and Palynology 109, 65–81.

Erba, E., 2004. Calcareous nannofossils and Mesozoic oceanic anoxic events. Marine Micropaleontology 52, 85–106.

Evitt, W.R., 1961. The dinoflagellate *Nannoceratopsis* Deflandre; morphology, affinities and infraspecific variability. Micropaleontology 7, 305–316.

Falkowski, P.G., Katz, M.E., Knoll, A.H., Quigg, A., Raven, J.A., Schofield, O., Taylor, F.J.R., 2004. The evolution of modern eukaryotic phytoplankton. Science 305, 354–360.

Farrimond, P., Eglinton, G., Brassell, S.C., Jenkyns, H.C., 1989. Toarcian anoxic event in Europe: An organic geochemical study. Marine and Petroleum Geology 6, 136–147.

Feist-Burkhardt, S., Götz, A., Ruckwied, K., Russel, J., 2008. Palynofacies patterns, acritarch diversity and stable isotope signatures in the Lower Muschelkalk (Middle Triassic) of N Switzerland: Evidence of third-order cyclicity. Swiss Journal of Geosciences 101, 1–15.

Feist-Burkhardt, S., Wille, W., 1992. Jurassic palynology in southwest Germany – state of the art. Cahiers de Micropaléontologie 7, 141–164.

Fensome, R.A., Williams, G.L., 2004. The Lentin and Williams index of fossil dinoflagellates. 2004 edition. American Association of Stratigraphic Palynologists Contributions Series No. 42, 909 p.

Fensome, R.A., Taylor, F.J.R., Norris, G., Sarjeant, W.A.S., Wharton, D.I., Williams, G.L., 1993. A classification of living and fossil dinoflagellates, Micropaleontology Press Special Paper 7, 351 p.

Galácz, A., 1991. Palaeontological investigation of the Toarcian black shale in the Mecsek Mts. Department of Palaeontology, Eötvös Loránd University, unpublished manuscript, 32 p.

Gocht, H., 1964. Planktonische Kleinformen aus dem Lias-/Dogger-Grenzbereich Nord- und Süddeutschlands. Neues Jahrbuch für Geologie und Paläontologie Abhandlungen 119, 113–133.

Gocht, H., 1972. Zur Morphologie der Dinoflagellaten-Gattung *Nannoceratopsis* Deflandre. Lethaia 5, 15–29.

Götz, A.E., Feist-Burkhardt, S., Ruckwied, K., 2008. Palynofacies and sea-level changes in the Upper Cretaceous of the Vocontian Basin, southeast France. Cretaceous Research 29, 1047–1057.

Grimm, E.C., 1987. CONISS: a FORTRAN 77 program for stratigraphically constrained cluster analysis by the method of incremental sum of squares. Computers and Geosciences 13, 13–35.

42

Grimm, E.C., 1991–2001. Tilia, TiliaGraph and TGView Software. Illinois State Museum, Springfield, Illinois, USA.

Guy-Ohlson, D., 1986. Jurassic palynology of the Vilhelmsfält bore No.1, Scania, Sweden Toarcian–Aalenian. Swedish Museum of Natural History, Stockholm, 127 p.

Haas, J., Péró, Cs., 2004. Mesozoic evolution of the Tisza Mega-unit. International Journal of Earth Sciences 93, 297–313.

Hammer, Ø., Harper, D.A.T., Ryan, P.D., 2001. PAST: palaeontological statistics software package for education and data analysis. Palaeontologica Electronica 4, 9.

Harries, P.J., Little, C.T.S., 1999. The early Toarcian (Early Jurassic) and the Cenomanian–Turonian (Late Cretaceous) mass extinctions: similarities and contrasts. Palaeogeography, Palaeoclimatology, Palaeoecology 154, 39–66.

Hermoso, M., Minoletti, F., Pellenard, P., 2013. Black shale deposition during Toarcian super-greenhouse driven by sea level. Climate of the Past 9, 2703–2712.

Hesselbo, S.P., Gröcke, D.R., Jenkyns, H.C., Bjerrum, C.J., Farrimond, P., Green, O.R., 2000. Massive dissociation of gas hydrate during a Jurassic oceanic anoxic event, Nature 406, 392–395.

Hesselbo, S.P., Jenkyns, H.C., Duarte, L.V., Oliveira, L.C.V., 2007. Carbon-isotope record of the Early Jurassic (Toarcian) Oceanic Anoxic Event from fossil wood and marine carbonate (Lusitanian Basin, Portugal). Earth and Planetary Science Letters 253, 455–470.

Hill, M.O., Gauch, H.G., 1980. Detrended correspondence analysis: an improved ordination technique. Vegetatio 42, 47–58.

Horváth, F., Galácz, A., 2006. The Carpathian-Pannonian Region. A Review of Mesozoic–Cenozoic Stratigraphy and Tectonics. Hantken Press, Budapest, 624 p.

Jenkyns, H.C., 1988. The early Toarcian (Jurassic) anoxic event; stratigraphic, sedimentary and geochemical evidence. American Journal of Science 288, 101–151.

Jenkyns, H.C., Gröcke, D.R., Hesselbo, S.P., 2001. Nitrogen isotope evidence for water mass denitrification during the early Toarcian (Jurassic) oceanic anoxic event. Paleoceanography 16, 1–11.

Jenkyns, H.C., Jones, C.E., Gröcke, D.R., Hesselbo, S.P., Parkinson, D.N., 2002. Chemostratigraphy of the Jurassic System: applications, limitations and implications for palaeoceanography. Journal of the Geological Society 159, 351–378.

Katz, M.E., Finkel, Z.V., Grzebyk, D., Knoll, A.H., Falkowski, P.G., 2004. Evolutionary

trajectories and biochemical impacts of marine eukaryotic phytoplankton. Annual Review of

Ecology, Evolution, and Systematics 35, 523–556.

Korte, C., Hesselbo, S.P., 2011. Shallow marine carbon and oxygen isotope and elemental

records indicate icehouse-greenhouse cycles during the Early Jurassic. Paleoceanography 26,

PA4219.

Kovach, W.L., 1993. Multivariate techniques for biostratigraphical correlation. Journal of the

Geological Society 150, 697–705.

Legendre, P., Legendre, L., 1998. Numerical Ecology. Elsevier Scientific, Oxford.

Littler, K., Hesselbo, S.P., Jenkyns, H.C., 2009. A carbon-isotope perturbation at the

Pliensbachian–Toarcian boundary: evidence from the Lias Group, NE England, Geological

Magazine 147, 181–192.

Loh, H., Maul, B., Prauss, M., Riegel, W., 1986. Primary production, maceral formation and

carbonate species in the Posidonia Shale of NW Germany. Mitteilungen des Geologisch-

Paläontologischen Institüts der Universität Hamburg 60, 397–421.

Lund, J.J., Pedersen, K.R., 1984. Palynology of the marine Jurassic formations in the Vardekløft ravine, Jameson Land, East Greenland. Bulletin of the Geological Society of Denmark 33, 371–400.

Marret, F., Zonneveld, K., 2003. Atlas of modern organic-walled dinoflagellate cyst distribution. Review of Palaeobotany and Palynology 125, 1–200.

Mattioli, E., Erba, E., 1999. Synthesis of calcareous nannofossil events in Tethyan Lower and Middle Jurassic succesions. Rivista Italiana di Paleontologia e Stratigrafia 105, 343–376.

Mattioli, E., Pittet, B., Bucefalo Palliani, R., Röhl, H.-J., Schmid-Röhl, A., Morettini, E., 2004. Phytoplankton evidence for the timing and correlation of palaeoceanographical changes during the early Toarcian oceanic anoxic event (Early Jurassic). Journal of the Geological Society 164, 685–693.

Mattioli, E., Pittet, B., Petitpierre, L., Maillot, S., 2009. Dramatic decrease of pelagic carbonate production by nannoplankton across the Early Toarcian anoxic event (T-OAE). Global and Planetary Change 65, 134–145.

McArthur, J.M., Donovan, D.T., Thirlwall, M.F., Fouke, B.W., Mattey, D., 2000. Strontium isotope profile of the early Toarcian (Jurassic) oceanic anoxic event, the duration of ammonite biozones, and belemnite palaeotemperatures. Earth and Planetary Science Letters 179, 269–285.

McDonald, J.H., 2014. Handbook of Biological Statistics (3rd edition). Sparky House Publishing, Baltimore, 305 p.

McElwain, J.C., Wade-Murphy, J., Hesselbo, S.P., 2005. Changes in carbon dioxide during an oceanic anoxic event linked to intrusion into Gondwana coals. Nature 435, 479–482.

Mertens, K.N., Bradley, L.R., Takano, Y., Mudie, P.J., Marret, F., Aksu, A.E., Hiscott, R.N., Verleye, T.J., Mousing, E.A., Smyrnova, L., Bagheri, S., Mansor, M., Pospelova, V., Matsuoka, K., 2012. Quantitative estimation of Holocene surface salinity variation in the Black Sea using dinoflagellate cyst process length. Quaternary Science Reviews 39, 45–59.

Némedi Varga, Z., 1998. Jurassic lithostratigraphy of the Mecsek and Villany. In: Bérczi, I., Jámbor, Á. (editors), Lithostratigraphic units in Hungary. Geological Institute of Hungary, Budapest, 319–336.

Oboh-Ikuenobe, F.E., de Villiers, S.E., 2003. Dispersed organic matter in samples from the western continental shelf of Southern Africa: palynofacies assemblages and depositional environments of Late Cretaceous and younger sediments. Palaeogeography, Palaeoclimatology, Palaeoecology 201, 67–88.

Pálfy, J., Smith, P.L., 2000. Synchrony between Early Jurassic extinction, oceanic anoxic event, and the Karoo-Ferrar flood basalt volcanism. Geology 28, 747–750.

Pittet, B., Gorin, G.E., 1997. Distribution of sedimentary organic matter in a mixed carbonate-siliciclastic platform environment: Oxfordian of the Jura Mountains. Sedimentology 44, 915–937.

Poulsen, N.E. 1992. Jurassic dinoflagellate cyst biostratigraphy of the Danish Subbasin in relation to sequences in England and Poland; a preliminary review. Review of Palaeobotany and Palynology 75, 33–52.

Poulsen, N.E., Riding, J.B., 2003. The Jurassic dinoflagellate cyst zonation of Subboreal Northwest Europe. Geological Survey of Denmark and Greenland Bulletin 1, 115–144.

Prauss, M., 1989. Dinozysten-Stratigraphie und Palynofazies im Oberen Lias und Dogger von NW-Deutschland. Palaeontographica Abteilung B, 214, 1–124.

Prauss, M., 1996. The Lower Toarcian Posidonia Shale of Grimmen, Northeast Germany. Implications from the palynological analysis of a near-shore section. Neues Jahrbuch für Geologie und Paläontologie Abhandlungen 200, 107–132.

Prauss, M., 2007. Availability of reduced nitrogene chemospecies in photic-zone waters as the ultimate cause for fossil prasinophyte prosperity. Palaios, 22, 489–499.

Prauss, M., Ligouis, B., Luterbacher, H.-P., 1991. Organic matter and palynomorphs in the ''Posidonienschiefer'' (Toarcian, Lower Jurassic) of southern Germany. In: Tyson, R.V., Pearson, T.H. (editors), Modern and Ancient Continental Shelf Anoxia. Geological Society of London Special Publication 58, 335–351.

Prauss, M., Riegel, W., 1989. Evidence from phytoplankton associations for causes of black shale formation in epicontinental seas. Neues Jahrbuch für Geologie und Paläontologie Monatshefte 11, 671–682.

Pross, J., 2001. Paleo-oxygenation in Tertiary epeiric seas: Evidence from dinoflagellate cysts. Palaeogeography, Palaeoclimatology, Palaeoecology 166, 369–381.

Raucsik, B., 2008. Apátvarasd, Réka Valley, opposite to the Disznós Spring, black shale outcrop. In: Galácz, A., Konrád, Gy., Raucsik, B., Vörös, A. (editors), Jurassic siliciclastics and carbonates of the Mecsek-Villány area. Field Trip Guide of the geological excursion on the Mecsek and Villány Hills. Hungarian Geological Society and the Sedimentological Subcommission of the Hungarian Academy of Sciences, 33–37.

Raucsik, B., 2012a. Vasas Marl Formation. In: Főzy, I. (editor), Jurassic lithostratigraphic units in Hungary. Hungarian Geological Society, 152–154.

Raucsik, B., 2012b. Hosszúhetény Calcareous Marl Formation. In: Főzy, I. (editor), Jurassic lithostratigraphic units in Hungary. Hungarian Geological Society, 155–158.

Raucsik, B., 2012c. Rékavölgy Siltstone Formation. In: Főzy, I. (editor), Jurassic lithostratigraphic units in Hungary. Hungarian Geological Society, 164–167.

Raucsik, B., 2012d. Komló Calcareous Marl Formation. In: Főzy, I. (editor), Jurassic lithostratigraphic units in Hungary. Hungarian Geological Society, 174–176.

Raucsik, B., Varga, A., 2008a. Climato-environmental controls on clay mineralogy of the Hettangian–Bajocian successions of the Mecsek Mountains, Hungary: Evidence for extreme continental weathering during the early Toarcian oceanic anoxic event. Palaeogeography, Palaeoclimatology, Palaeoecology 265, 1–13.

Raucsik, B., Varga, A., 2008b. Mineralogy of the Lower Toarcian black shale section from the Réka Valley (Óbánya Siltstone Formation, Mecsek Mountains, Hungary): implications for palaeoclimate. Földtani Közlöny 138, 133–146.

Riding, J.B., 1983. The palynology of the Aalenian (Middle Jurassic) sediments of Jackdaw Quarry, Gloucestershire, England. Mercian Geologist 9, 111–120.

Riding, J.B., 1984. A palynological investigation of Toarcian to early Aalenian strata from the Blea Wyke area, Ravenscar, North Yorkshire. Proceedings of the Yorkshire Geological Society 45, 109–122.

Riding, J.B., 1987. Dinoflagellate cyst stratigraphy of the Nettleton Bottom Borehole (Jurassic: Hettangian to Kimmeridgian) Lincolnshire, England. Proceedings of the Yorkshire Geological Society 46, 231–266.

Riding, J.B., Thomas, J.E., 1992. Dinoflagellate cysts of the Jurassic System. In: Powell, A.J. (editor), A stratigraphic index of dinoflagellate cysts, British Micropalaeontological Society Publications Series, 7–97.

Riding, J.B., Penn, I.E., Woollam, R., 1985. Dinoflagellate cysts from the type area of the Bathonian Stage (Middle Jurassic; south-west England). Review of Palaeobotany and Palynology 45, 149–170.

Rochon, A., Lewis, J., Ellegaard, M., Harding, I.C., 2009. The *Gonyaulax spinifera* (Dinophyceae) "complex": Perpetuating the paradox? Review of Palaeobotany and Palynology 155, 52–60.

Röhl, H.-J., Schmid-Röhl, A., 2005. Lower Toarcian (Upper Liassic) black shales of the Central European epicontinental basin: a sequence stratigraphic case study from the SW Germany, Posidonia Shale. SEPM Special Publications 82, 165–189.

51

Schouten, S., van Kaam-Peters, H.M.E., Rijpstra, W.I.C., Schoell, M., Sinnighe Damaste, J.S., 2000. Effects of an anoxic event on the stable carbon isotope composition of Early Toarcian carbon. American Journal of Science 300, 1–22.

Stover, L.E., Brinkhuis, H., Damassa, S.P., de Verteuil, L, Helby, R.J., Monteil, E., Partridge, A.D., Powell, A.J., Riding, J.B., Smelror, M., Williams, G.L., 1996. Mesozoic-Tertiary dinoflagellates, acritarchs and prasinophytes. In: Jansonius, J., McGregor, D.C. (editors), Palynology: Principles and Applications. American Association of Stratigraphic Palynologists Foundation 2, 641–750.

Suan, G., Mattioli, E., Pittet, B., Maillot, S., Lécuyer, C., 2008. Evidence for major environmental perturbation prior to and during the Toarcian (Early Jurassic) oceanic anoxic event from the Lusitanian Basin, Portugal. Paleoceanography 23, PA1202.

Svensen, H., Planke, S., Chevallier, L., Malthe-Sørenssen, A., Corfu, F., Jamtveit, B., 2007. Hydrothermal venting of greenhouse gases triggering Early Jurassic global warming. Earth and Planetary Science Letters 256, 554–566.

Szente, I., 2012. Mecsek Coal Formation. In: Főzy, I. (editor), Jurassic lithostratigraphic units in Hungary. Hungarian Geological Society, 145–148.

Taylor, F.J.R., Hoppenrath, M., Saldarriaga, J.F., 2008. Dinoflagellate diversity and distribution. Biodiversity and Conservation 17, 407–418.

Tyson, R.V., 1993. Palynofacies analysis. In: Jenkins, D.G. (editor), Applied Micropaleontology. Kluwer Academic Publishers, The Netherlands, 153–191.

Tyson, R.V., 1995. Sedimentary organic matter: organic facies and palynofacies. Chapman and Hall, London, 615 p.

Van de Schootbrugge, B., Bachan, A., Suan, G., Richoz, S., Payne, J.L., 2013. Microbes, mud and methane: cause and consequence of recurrent Early Jurassic anoxia following the end-Triassic mass extinction. Palaeontology 56, 685–709.

Van de Schootbrugge, B., McArthur, J.M., Bailey, T.R., Rosenthal, Y., Wright, J.D., Miller, K.G., 2005a. Toarcian oceanic anoxic event: assessment of global causes using belemnite C-isotope records. Paleoceanography 20, PA3008.

Van de Schootbrugge, B., Bailey, T.R., Rosenthal, Y., Katz, M.E., Wright, J.D., Miller, K.G., Feist-Burkhardt, S., Falkowski P.G., 2005b. Early Jurassic climate change and the radiation of organic-walled phytoplankton in the Tethys Ocean. Paleobiology 31, 73–97.

Van de Schootbrugge, B., Quan, T.M., Lindström, S., Püttmann, W., Heunisch, C., Pross, J., Fiebig, J., Petschick, R., Röhling, H., Richoz, H.-G., Rosenthal, Y., Falkowski, P.G. 2009. Floral changes across the Triassic–Jurassic boundary linked to flood basalt volcanism. Nature Geoscience 2, 589–594.

Van Erve, A.W., 1977. Palynological investigation in the Lower Jurassic of the Vicentinian Alps (Northeastern Italy). Review of Palaeobotany and Palynology 23, 1–117.

Varga, A., Mikes, T., Raucsik, B. 2009. The petrography and heavy minerals of the Toarcian black shale of the Réka Valley section of the Mecsek Hills: a pilot study. Földtani Közlöny 139, 31–53.

Varga, A.R., Raucsik, B., Hámor-Vidó, M., Rostási, A., 2007. Isotope geochemistry and characterization of hydrocarbon potential of black shale from Óbánya Siltstone Formation. Földtani Közlöny 137, 449–472.

Verleye, T.J., Mertens, K.N., Young, M.D., Dale, B., McMinn, A., Scott, L., Zonneveld, K.A.F., Louwye, S., 2012. Average process length variation of the marine dinoflagellate cyst *Operculodinium centrocarpum* in the tropical and Southern Hemisphere Oceans: Assessing its potential as a palaeosalinity proxy. Marine Micropaleontology 86–87, 45–58.

Wall, D., 1965. Microplankton, pollen, and spores from the Lower Jurassic in Britain. Micropaleontology 11, 151–190.

Wall, D., Dale, B., Lohmann, G.P., Smith, W.K. 1977. The environmental and climatic distribution of dinoflagellate cysts in modern marine sediments from regions in the North and south Atlantic oceans and adjacent seas. Marine Micropaleontology 2, 121–200.

Wignall, P.B., 2001. Large igneous provinces and mass extinctions. Earth-Science Reviews 53, 1–33.

Wignall, P.B., Benton, M.J., 1999. Lazarus taxa and fossil abundances at times of biotic crisis. Journal of the Geological Society of London 156, 453U456.

Wille, W., 1982. Ecology and evolution of Upper Liassic dinoflagellates from SW Germany. Neues Jahrbuch für Geologie und Paläontologie Abhandlungen 164, 74–82.

Woollam, R., Riding, J.B. 1983. Dinoflagellate cyst zonation of the English Jurassic. Institute of Geological Sciences Report 83/2, 1–44.

Wood, G.D., Gabriel, A.M., Lawson, J.C., 1996. Palynological techniques – processing and microscopy. In: Jansonius, J., McGregor, D. C. (editors), Palynology: Principles and Applications. American Association of Stratigraphic Palynologists Foundation 1, 29–50.

Display material captions:

Fig. 1. A. The geological framework and the major tectonic units of the Carpathian–Pannonian area (after Csontos and Vörös, 2004). The box indicates the area shown in 1B. B. Generalised geological map of the Mecsek Mountains, southwest Hungary illustrating the outcrop area of the Jurassic formations. The location of the Réka Valley section is marked by an asterisk. Modified after Raucsik and Varga (2008a), with structural geology from Csontos et al. (2002).

Fig. 2. Early Jurassic palaeogeography of the western Neotethys and adjacent epicontinental areas, showing the position of the area studied and the other occurrences of lower Toarcian black shale discussed in the text (Jenkyns, 1988). Modified after Varga et al. (2007); base map after Bassoulet et al. (1993).

Fig. 3. Lithostratigraphy of the Lower and Middle Jurassic formations of the Mecsek Mountains, southwest Hungary, indicating their depositional setting (modified after Raucsik and Varga, 2008a).

Fig. 4. Location map of the section investigated (above), and a close-up photograph of the outcrop (below). Key: 1 – creek; 2 – trail; 3 – road; 4 – settlement. Modified after Raucsik and Varga (2008b).

Fig. 5. A. Lithological log of the Réka Valley section showing the positions of the palynomorph samples (modified after Galácz, 1991). B. Detailed lithological log of the black shale interval, modified after Raucsik and Varga (2008b) and Varga et al. (2009).

Fig. 6. Simpson Diversity Index and the relative proportions of the different palynomorph groups in the Réka Valley section. The abundance of palynomorphs is given in percentages. The group "Other dinoflagellate cysts" includes *Mancodinium semitabulatum*, *Mendicodinium* sp., *Umbriadinium mediterranense* and *Valvaeodinium* sp.; the low abundances of these forms does not permit their separate plotting. The lithological log on the left is not to scale. The grey shaded area has an exaggeration factor of X2.

Fig. 7. Palynofacies results and the values of the different palynofacies indices in the section studied. No indices were calculated for samples from the black shale unit because of the overwhelming dominance of amorphous organic matter (AOM) that hindered the counting of any other organic particles. The following palynofacies indices are shown: ratio of terrestrial to marine palynomorphs (t/m); ratio of spores to bisaccate pollen grains (sp/bs); ratio of opaque to translucent phytoclasts (o/t); ratio of bladded-lath shaped to equidimensional opaque phytoclasts (bl/eq). The lithological log on the left is not to scale.

Fig. 8. A: Scatter plot of correspondence analysis (CA) and B: scatter plot of detrended correspondence analysis (DCA) performed on the samples from the Réka Valley section. Note palaeoecologically controlled differences among the palynomorph assemblages. See text for details.

Fig. 9. Comparison of the palynomorph records and biotic events from five localities, including the Réka Valley section. Based on Prauss (1989; 1996; 2007), Prauss et al. (1991), Bucefalo Palliani and Riding (1997a; 1999a) and Bucefalo Palliani et al. (1998; 2002).

Table 1. Summary of palynofacies terminology and the different palynofacies indices. The terminology used is from Oboh-Ikuenobe and de Villiers (2003), Feist-Burkhardt et al. (2008) and Götz et al. (2008).

Plate I. Dinoflagellate cysts from the Réka Valley section. The scale bar represents 20 µm. Sample number and slide numbers are given in square brackets after the name.

1. *Nannoceratopsis senex* van Helden 1977 [RV 10/1].

2. *Nannoceratopsis gracilis* Alberti 1961 [RV 8/2].

3. *Nannoceratopsis gracilis* Alberti 1961 [RV 9/2]

4. *Nannoceratopsis gracilis* subsp. *obsoleta* (Prauss 1989) Lentin & Williams 1993 [RV 8/1].

5. *Nannoceratopsis gracilis* subsp. *obsoleta* (Prauss 1989) Lentin & Williams 1993 [RV 8/1].

6. *Nannoceratopsis* sp. [RV 9/2].

7. *Nannoceratopsis gracilis* Alberti 1961 [RV 9/2]

8. *Nannoceratopsis gracilis* Alberti 1961 [RV 2/1]

9. *Luehndea microreticulata* Bucefalo Palliani et al. 1997 [RV 4/1].

10. *Luehndea microreticulata* Bucefalo Palliani et al. 1997 [RV 4/2].

11. *Nannoceratopsis* sp. cf. *N. magnicornus* Bucefalo Palliani & Riding 1997 [RV 8/1].

12. *Luehndea spinosa* Morgenroth 1970 [RV 9/1].

13. *Nannoceratopsis spiculata* Stover 1966 [RV 20/1].

Plate II. Pollen and spores from the Réka Valley section. The scale bar represents 20 μm unless otherwise indicated. Sample number and slide numbers are given in square brackets after the name.

1. *Contignisporites problematicus* (Couper 1953) Döring 1965 [RV 11/2].

2. *Ischyosporites variegatus* Couper 1958 [RV 11/2].

3. *Cingutriletes* sp. [RV 18/1].

4. *Cibotiumspora jurienensis* (Balme 1957) Filatoff 1965 [RV 11/2].

5. *Dictyophyllidites harrisii* Couper 1958 [RV 11/2].

6. *Auritulinasporites triclavis* Nilsson 1958 [RV 8/2].

7. *Cyathidites australis* Couper 1953 [RV 4/1]; scale bar = 30 μm.

8. *Neoraistrickia* sp. [RV 16/1].

9. *Osmundacidites wellmanii* Couper 1953 [RV 11/1].

10. *Manumia delcourtii* (Pocock 1970) Dybkjær 1991 [RV 16/1].

11. *Baculatisporites* sp. [RV 8/2].

12. *Concavisporites toralis* (Leschik 1955) Nilsson 1958 [RV 3/1].

13. *Classopollis* sp. [RV 7/1].

14. *Alisporites robostus* Nilsson 1958 [RV 1/1]; scale bar = 30 μm.

15. *Spheripollenites psilatus* Couper 1958 [RV 13/1]; scale bar = 50 μm.

16. *Classopollis* sp. [RV 3/2].

17. *Alisporites* sp. cf. *A. thomasii* (Couper 1958) Nilsson 1958 [RV 4/2].

18. *Chasmatosporites* sp. [RV 3/2].

19. *Monosulcites minimus* Cookson 1947 [RV 3/2].

Plate III. Sphaeromorphs and representative palynofacies from the Réka Valley section.

1. Sphaeromorphs in clusters. Sample BS 32; scale bar = 20 μm.

2. Sphaeromorphs in clusters. Sample BS 56; scale bar = 20 μm.

3. Fluorescence photomicrograph of amorphous organic material (AOM). The particles with higher fluorescence intensities are palynomorphs, the phytoclasts are masked by AOM; scale bar = 50 μm.

4. Palynofacies of Assemblage 3 with predominant AOM; scale bar = 100 μm.

5. Palynofacies of Assemblage 1 with predominant translucent phytoclasts; scale bar = 100 μm.

6. Palynofacies of Interval 2 with *Nannoceratopsis* sp. from Plate I, fig. 6; scale bar = 100 μm.

7. Palynofacies of Interval 4 with high levels of translucent phytoclasts; scale bar = 100 μm.

8. Palynofacies of Interval 5 with predominant opaque, equidimensional phytoclasts; scale bar = 100 μm.

A

Alpine–Carpathian flysch belt

Inner Alpine–Carpathian Mountain belt and the Dinarides

border of Hungary

Pieniny Klippen belt

Neogene calc-alkaline volcanic rocks

B

Carboniferous granite

Permian rhyolite

Permian sedimentary rocks

Triassic carbonates

Jurassic sedimentary rocks

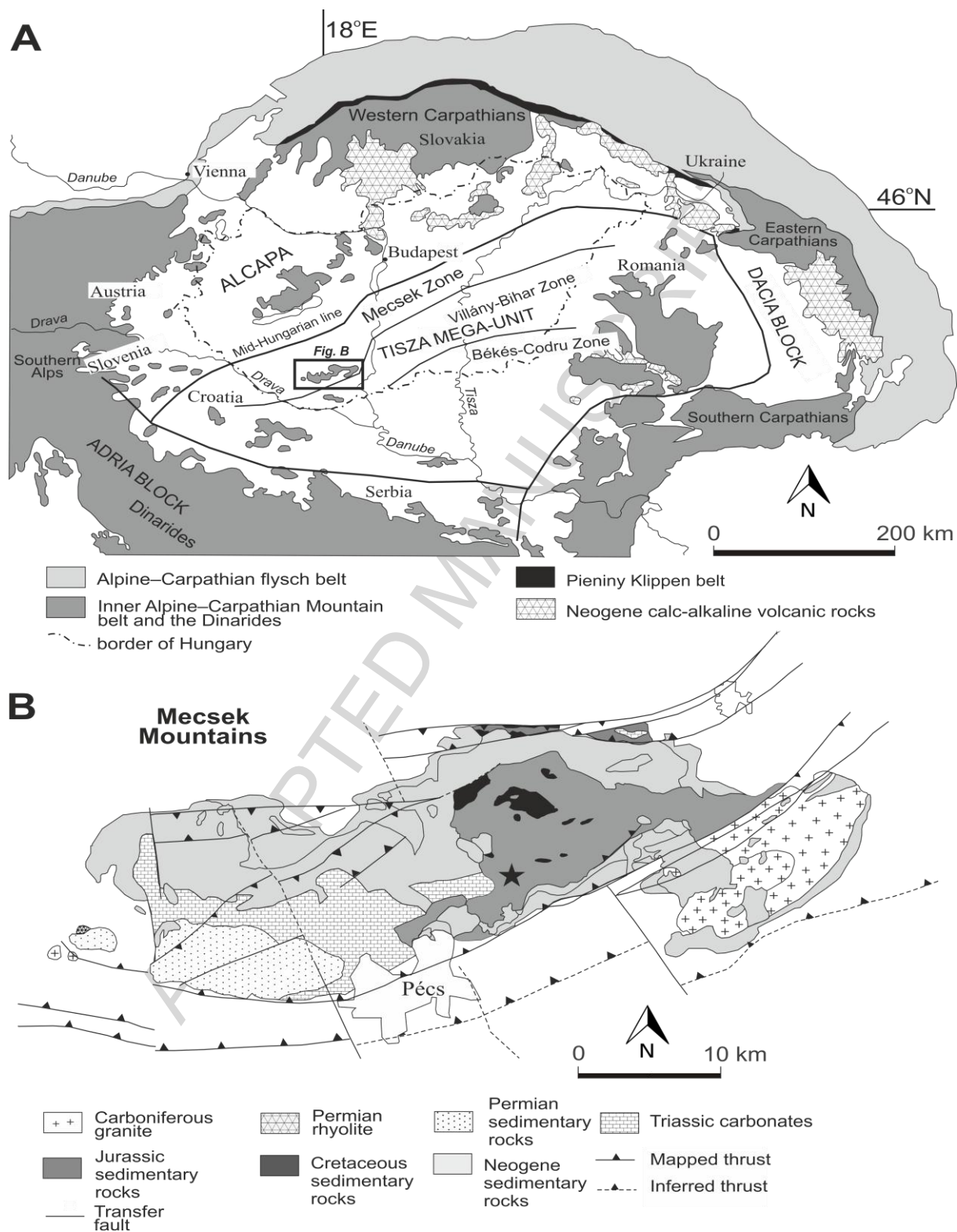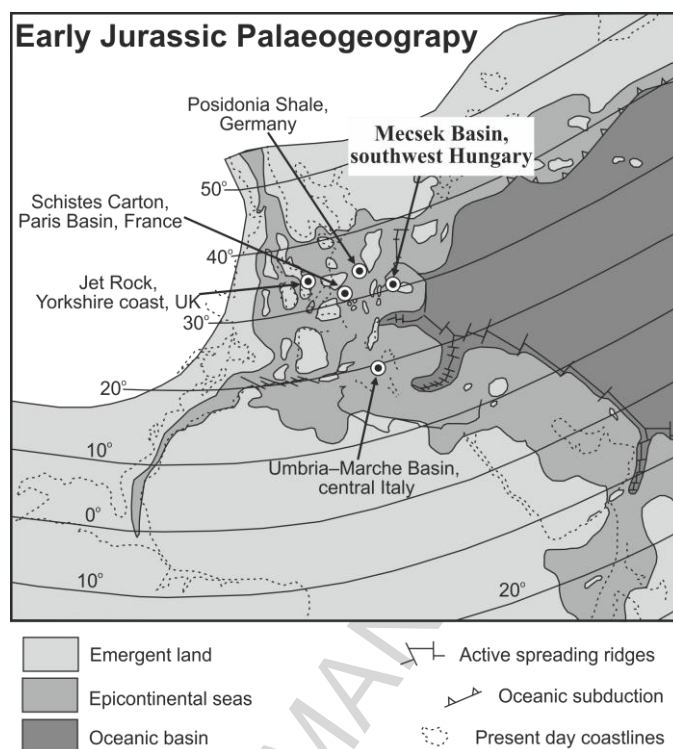Cretaceous sedimentary rocks
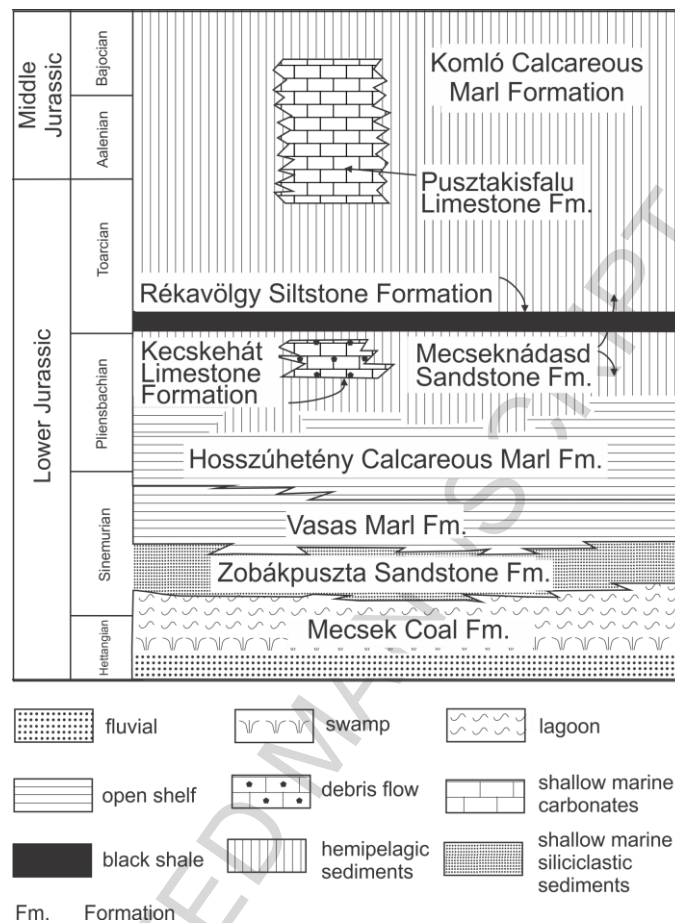
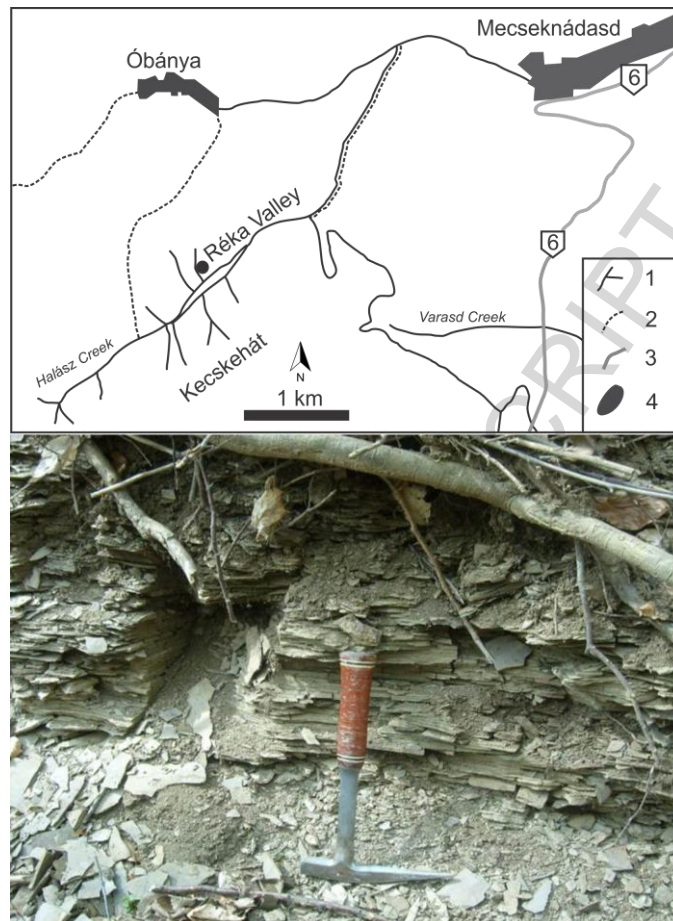Neogene sedimentary rocks

Mapped thrust

Inferred thrust

Transfer fault

Figure 1

Figure 2

Figure 3

Figure 4
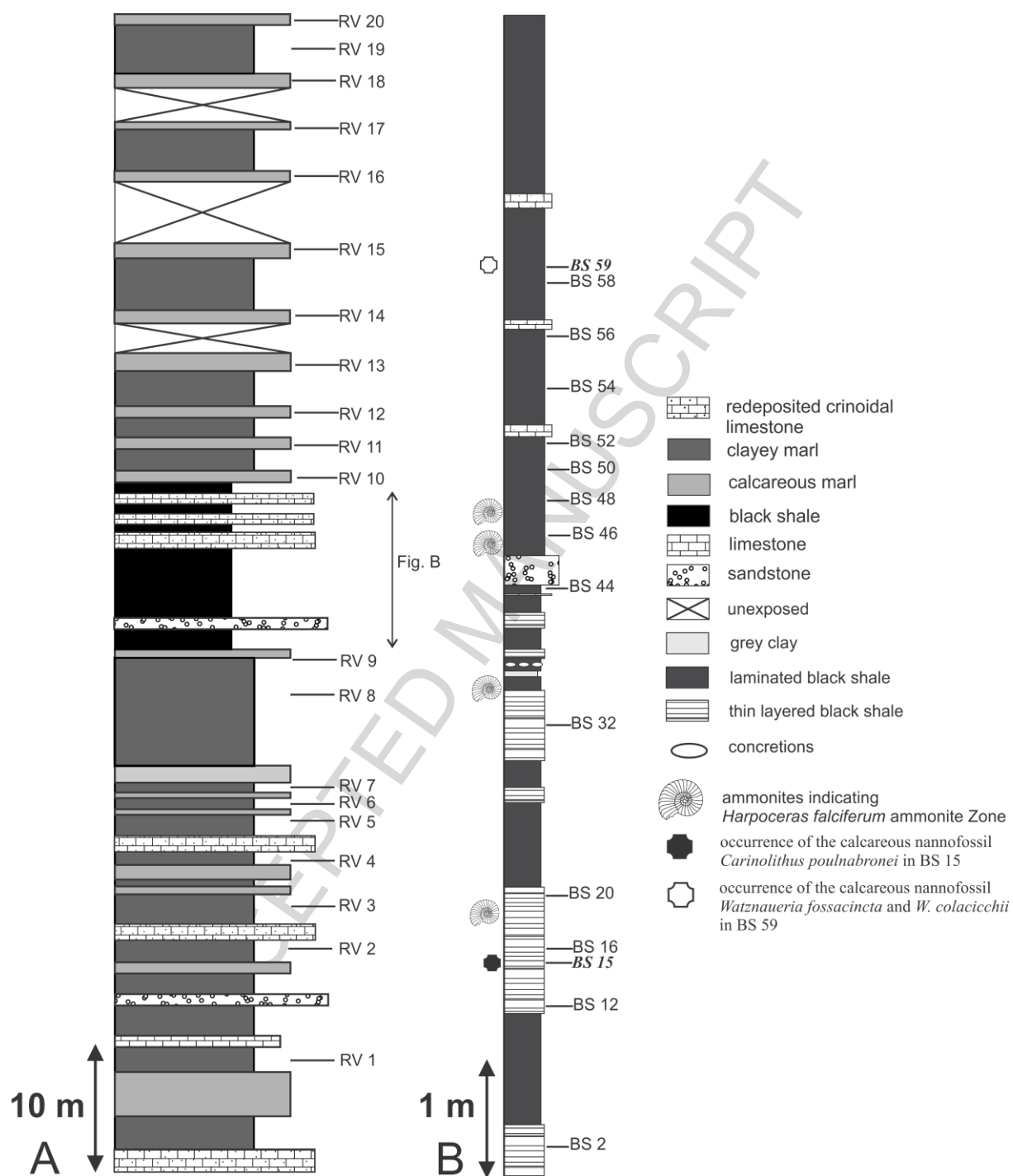
Figure 5

Figure 6

Figure 7

67
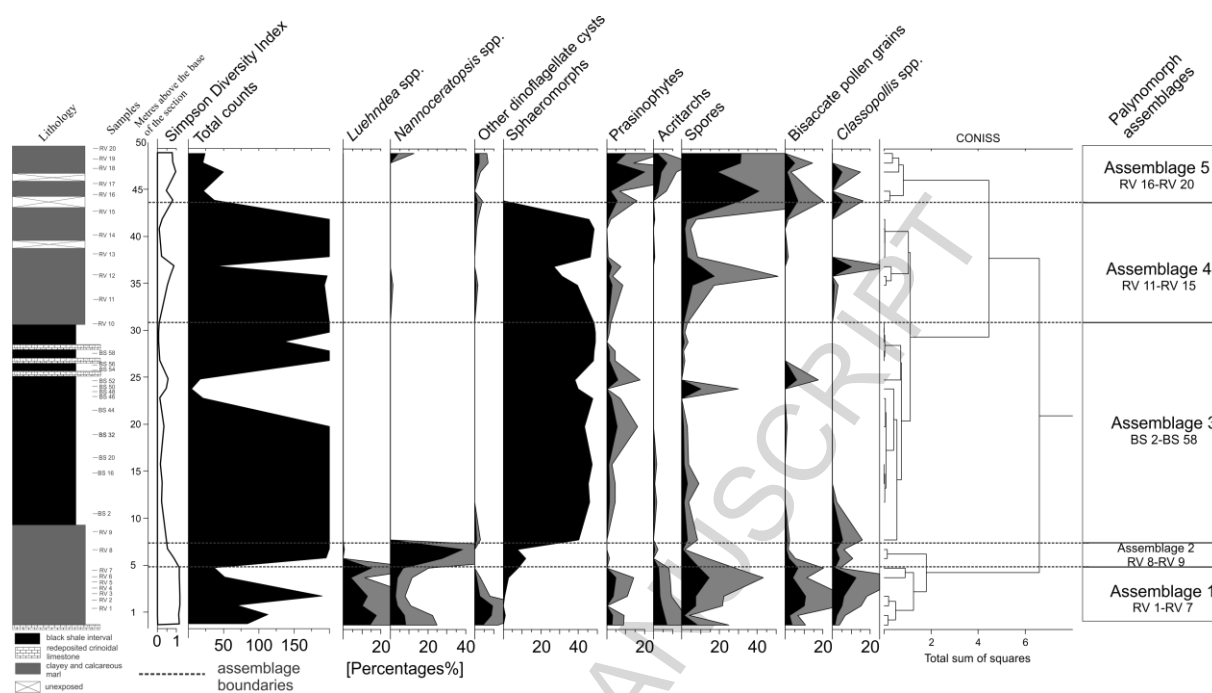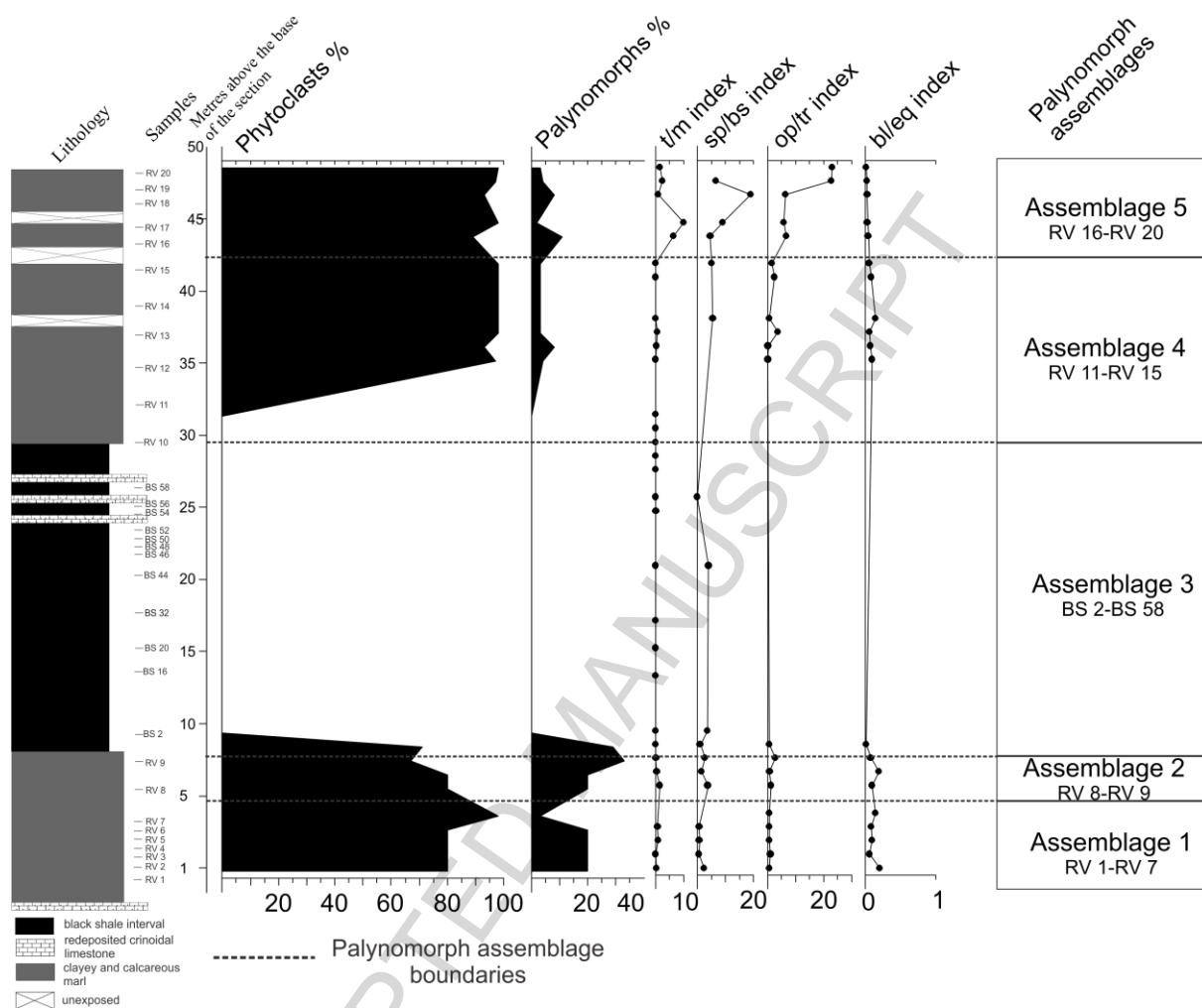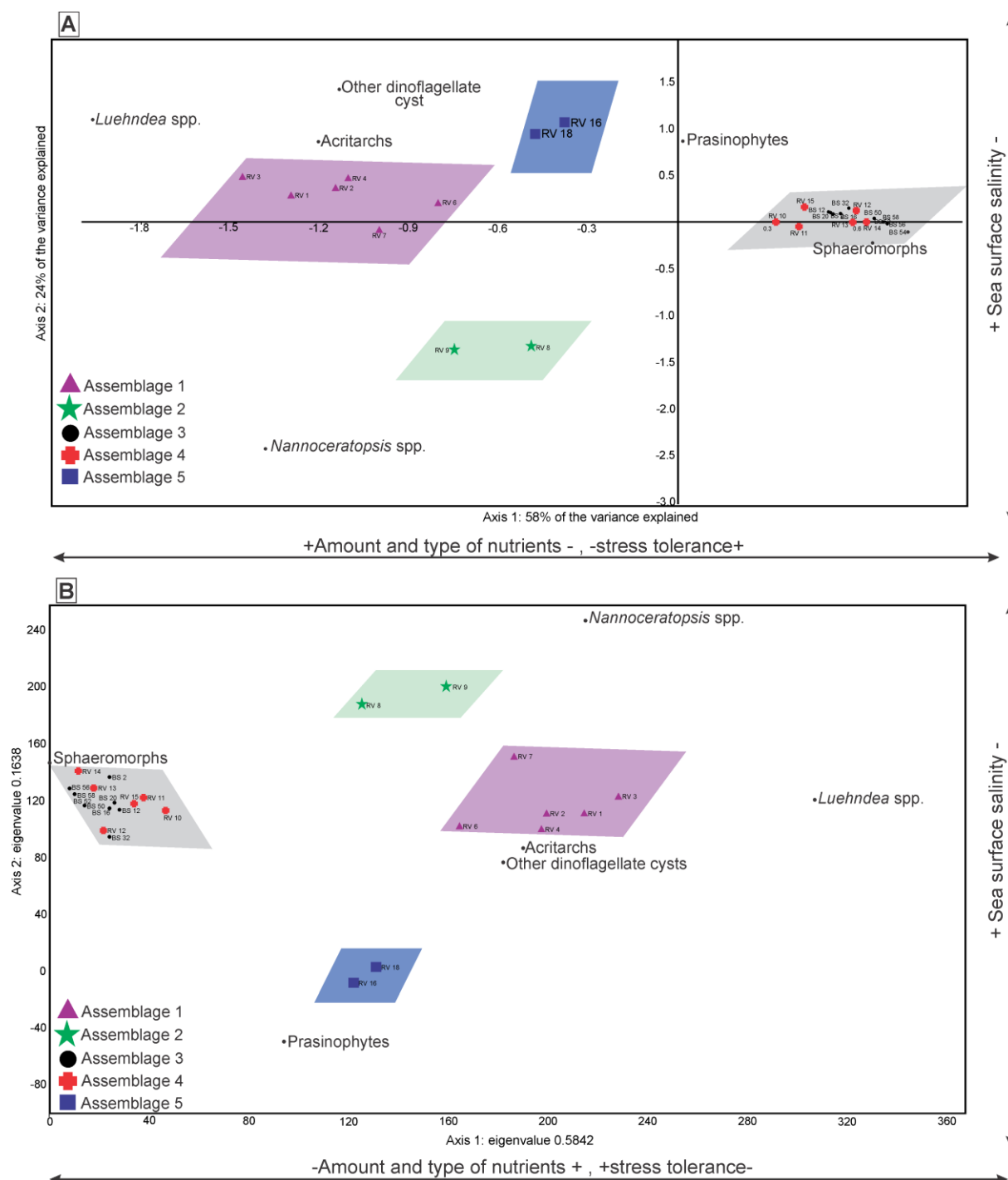
Figure 8

68

Biostratigraphy		Biotic events & characteristic organic-walled phytoplankton groups				
Ammonite biozones and subbiozones		**Réka Valley** Hungary (this study)	**Posidonia Shale** NW and SW Germany (Prauss, 1989, 1996; Prauss et al., 1991)	**Yorkshire** England (Bucefalo Palliani et al., 2002)	**Quercy** (SW France) (Bucefalo Palliani & Riding, 1997a)	**Umbria-Marche Basin** Central Italy (Bucefalo Palliani et al., 1998; Bucefalo Palliani & Riding, 1999a)
H. bifrons Zone		recovery Interval 4-5	recovery	recovery	no data	no data
H. falciferum Zone	*H. falciferum* Subzone / *H. exaratum* Subzone	Dinoflagellate cyst blackout — Sphaeromorphs and *Tasmanites* — Interval 3	Dinoflagellate cyst blackout — Sphaeromorphs and *Tasmanites*	survival — reappearance of *Nannoceratopsis* / *Tasmanites* Sphaeromorphs / Dinoflagellate cyst blackout Sphaeromorphs	no data	no data
D. tenuicostatum Zone	*D. semicelatum* Subzone	LO of *L. spinosa* *Nannoceratopsis* spike Interval 2	LO of *L. spinosa* — *Nannoceratopsis senex* dominance	*Nannoceratopsis* dominance	*Nannoceratopsis* dominance	Phase 4 **recovery** *Susadinium* and *Mendicodinium*
	D. clev. S.					Phase 3 Dinoflagellate cyst blackout *Tasmanites* and sphaeromorphs
	P. paltus Subzone	*Luehndea* dominance Interval 1	*L. spinosa* dominance		*Luehndea* dominance	Phase 2 *Umbriadinium* and *Valveodinium*
						Phase 1 *Luehndea* and *Mancodinium*
P. spinatum Zone		no data	*Nannoceratopsis gracilis* dominance			no data

· · · · · · biostratigraphical assignment uncertain

Figure 9

69

Plate I

Plate II

71
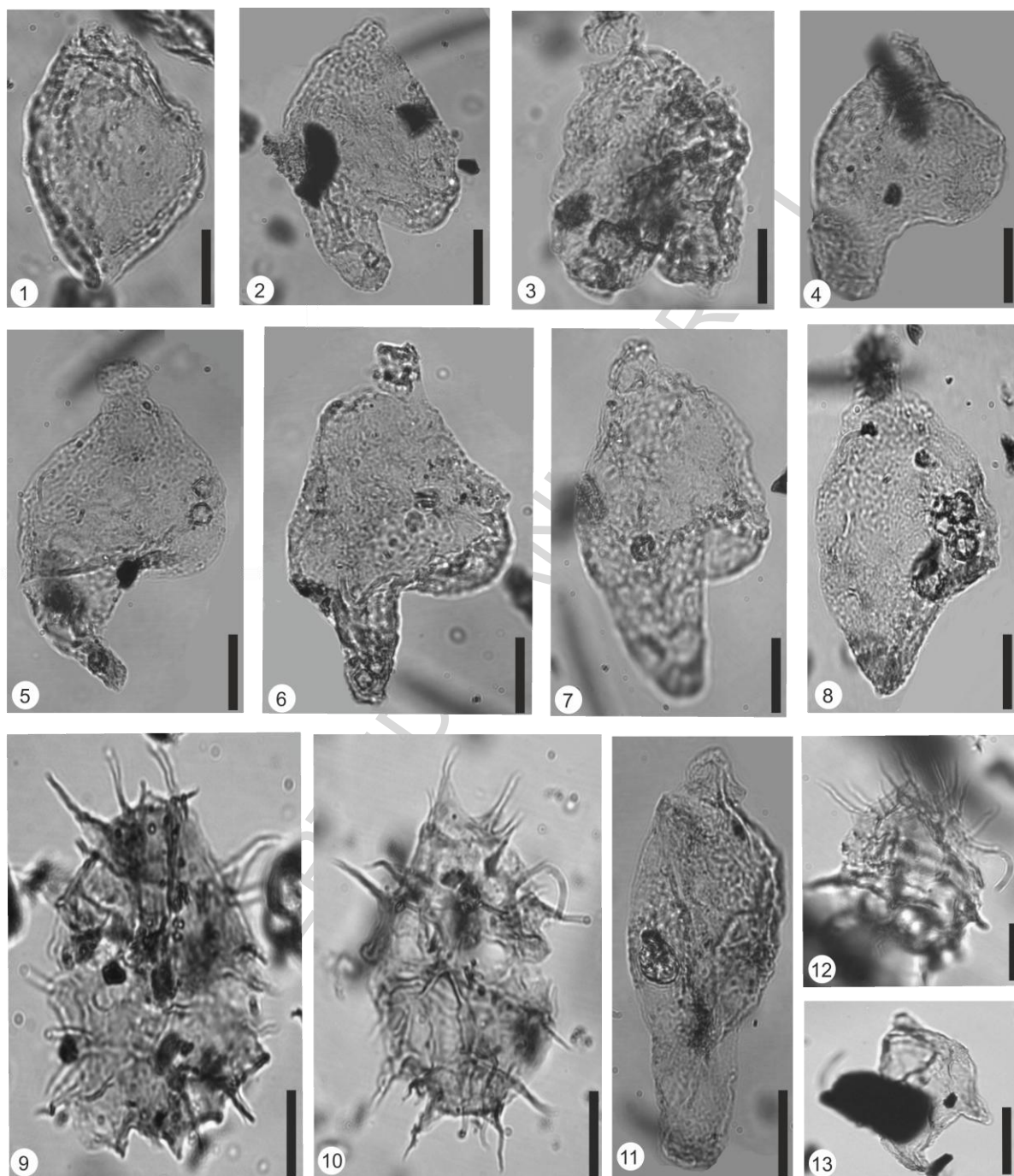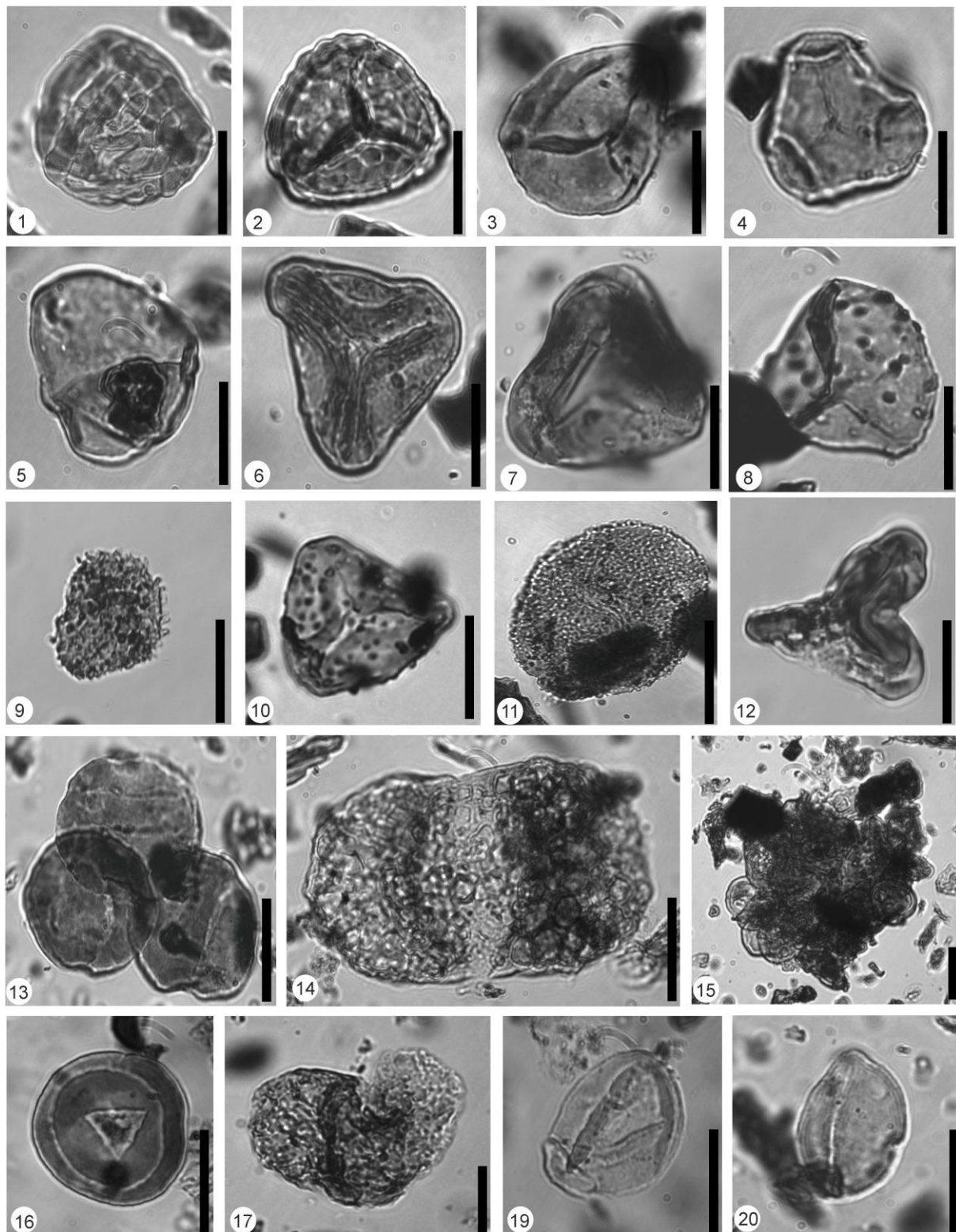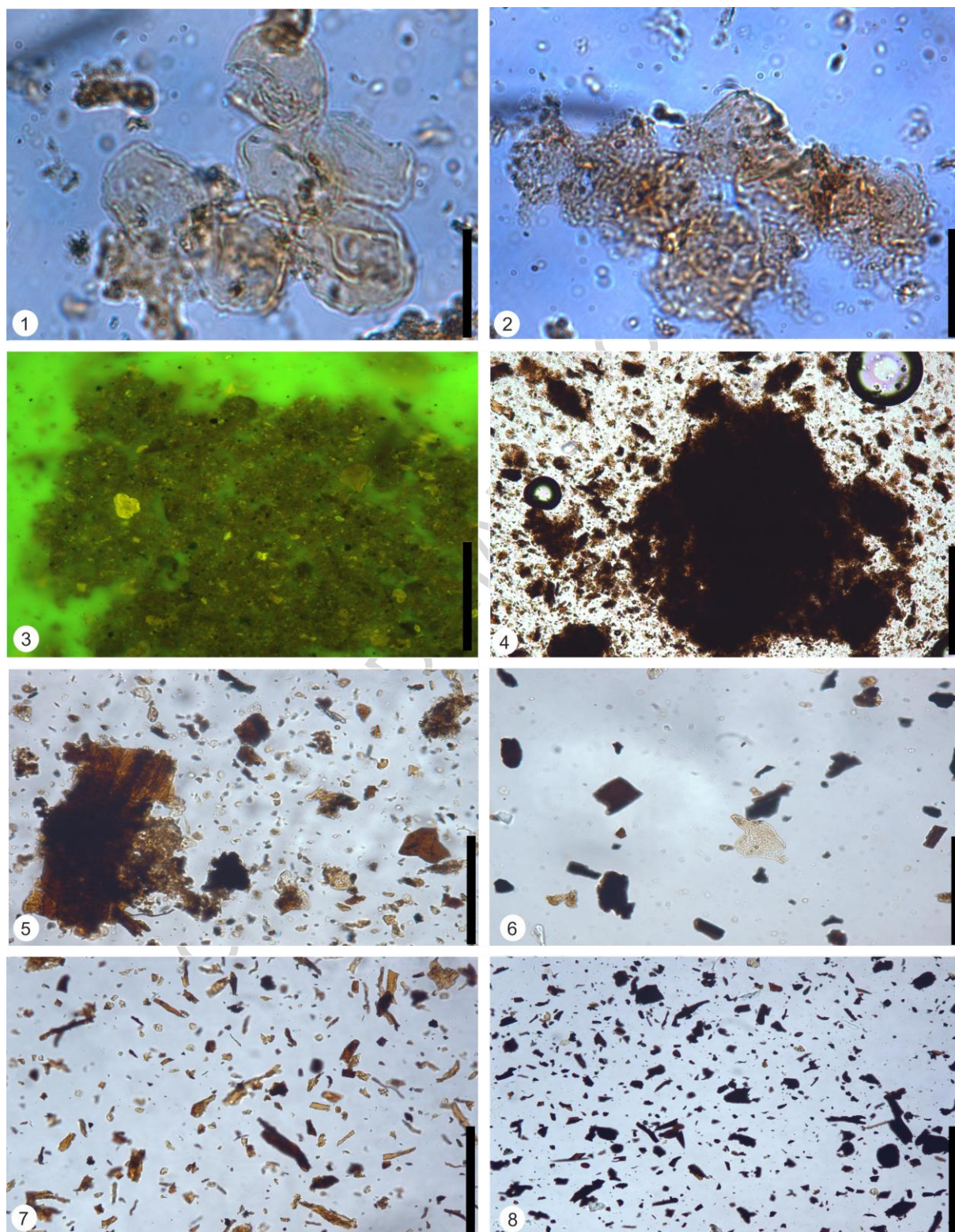
Plate III

Table 1
Palynofacies terminology

Sedimentary organic particles	Description
Amorphous organic matter (AOM)	Structureless, irregularly shaped, fluffy yellowish-brown to black masses that can be derived from the degradation of terrestrial or marine organic matter
Charcoal/black debris	Totally opaque particles with variable shape and size. They are derived from highly oxidised wood or other plant debris.
Structured translucent plant debris	Structured transparent particles with yellow-green to brown colour. They may be derived from degraded plant tissues or wood. They are of various shape and size including lath-shaped and equidimensional particles. As cuticles are extremely scarce in the investigated material, they were counted as part of this group.
Spores	Male reproductive organs of bryophytes and pteridophytes
Pollen grains	Male reproductive organs of the seed plants
Marine palynomorphs	Dinoflagellate cysts, acritarchs, prasinophytes, sphaeromorphs and chitinous inner linings of foraminifera

Palynofacies indices

t/m index	The t/m index quantifies the ratio of terrestrial (t) to marine (m) palynomorphs, which reflects the vegetation of the hinterland and the proportion of terrigenous input
sp/bs index	The sp/bs index measures the ratio of spores (sp) to bisaccate pollen grains (bs)
op/tr index	The op/tr index quantifies the ratio of opaque (op) to translucent (tr) phytoclasts. It can indicate changes in the depositional environment, as it reflects shifts between proximal and distal settings.
bl/eq index	The bl/eq index measures the ratio of bladed-lath shaped (bl) and equidimensional (eq) opaque phytoclasts, which also captures proximal/distal trends.

73

Highlights

- Detailed quantitative palynological analysis of a Toarcian black shale succession

- Five successive intervals recorded changes in organic-walled phytoplankton assemblages

- Peak of the euryhaline dinoflagellate *Nannoceratopsis*, followed by a blackout event

- Changes driven by global warming, enhanced runoff and freshening of surface waters